



WPI

Fabrication and Characterization of Asymmetric Phosphoinositide-Containing Vesicles

A Major Qualifying Project Report Submitted to the Faculty of
WORCESTER POLYTECHNIC INSTITUTE
In partial fulfillment of the requirements for the
Degree of Bachelor of Science in Biochemistry

Written by:

Olivia Hunker

Approved by:

Dr. Arne Gericke

May 2020

Table of Contents

Acknowledgements.....	3
Abstract.....	4
1. Introduction.....	5
2. Background.....	6
2.1 Biological Membrane Structure.....	6
2.1.1 Lipid Rafts.....	6
2.1.2 Model Membranes.....	7
2.1.3 Asymmetric Model Membranes.....	8
2.2 Phosphoinositides and PI(4,5)P ₂	8
2.2.1 Lateral Organization of PI(4,5)P ₂	9
2.2.3 PI(4,5)P ₂ Signaling Events are Linked to Lipid Rafts.....	10
2.2.4 Coupling of Phosphoinositide Domains and Lipid Raft Domains.....	10
2.3 Hypothesis.....	10
3. Methodology.....	11
4. Results.....	14
4.1 Electroformation of GUVs can be carried out in low and high salt.....	14
4.2 Fluorescence recovery after photobleaching confirms supported lipid bilayer formation.....	16
4.3 Hemifusion is a viable method to form phosphoinositide-containing aGUVs.....	16
4.4 Calcium concentration.....	18
5. Discussion.....	18
5.1 Symmetric GUV formation.....	18
5.2 Differences between SLBs formed from SUVs and LUVs.....	19
5.3 Phase separated versus non-phase separated vesicles.....	19
5.4 Characteristics of phosphoinositide-containing aGUVs.....	20
5.5 Future directions.....	21
6. Conclusion.....	23
Tables and Figures.....	24
References.....	34

Acknowledgements

I would like to thank my advisors Dr. Arne Gericke for his support and for allowing me to work in his lab. I would like to thank Dr. Alonzo Ross for his advice and guidance throughout this project. I would also like to thank Gericke group members Karin Plante, Dr. Anne-Marie Bryant, and Dr. V. Siddartha Yerramilli for their help and guidance in the lab. I'd like to thank the Scarlata group for use of their confocal microscope. I especially thank Dr. Thais Enoki for her guidance on the hemifusion method and for providing the code for analyzing GUV fluorescence intensity. Lastly, I would like to thank my friends and family for supporting me throughout my undergraduate career.

Abstract

The composition of biological membranes is laterally heterogeneous and vertically asymmetric. It is widely accepted that liquid-ordered (l_o) domains (lipid rafts) occur in biological membranes. While lipid raft domains have been widely investigated in *in vitro* systems, these systems have not incorporated the vertical asymmetry of biological membranes. Recently, methodologies to fabricate vertically asymmetric vesicles have emerged to remedy this deficiency. Experimental evidence has linked phosphoinositide (PIP) mediated signaling events to lipid rafts, and it has been speculated that PIPs accumulate in rafts. Interactions between lipid rafts and PIPs would provide an efficient mechanism for the regulation of PIP-mediated signaling events in cellular membranes. However, the acyl chain composition of PIPs is unfavorable for accumulation in the l_o environment of rafts, and PIPs do not enrich in l_o phases in symmetric vesicles. Despite this, it has been shown that cholesterol promotes PIP domain formation in ternary PC/PIP/cholesterol lipid mixtures, presumably through a stabilizing interaction between the PIP headgroup and cholesterol hydroxyl group. Additionally, experiments with asymmetric vesicles have shown that the phase behavior in opposing leaflets can exert influence on each other, an interaction that is called interleaflet coupling. To investigate the potential coupling of outer leaflet raft domains and inner leaflet PIP/cholesterol domains, an asymmetric PI(4,5)P₂-containing vesicle system was established and characterized. This system can be used to characterize interactions between l_o domains and PIP domains under various conditions.

1. Introduction

Phosphoinositides are a class of membrane lipids that mediate many cellular signaling pathways including cell communication, cell survival and proliferation, host-pathogen interactions, cytoskeleton organization, membrane trafficking, and gene expression. Dysregulation of these pathways are associated with disease states such as cancer and diabetes [1]. The phosphoinositide species phosphatidylinositol-4,5-bisphosphate (PI(4,5)P₂) is found in the inner leaflet of the plasma membrane. Several studies have linked PI(4,5)P₂-mediated signaling pathways to the presence of lipid rafts [2-10], suggesting that an interaction between lipid rafts and PI(4,5)P₂ is involved in the regulation of these pathways.

Lipid rafts are membrane domains that have distinct composition from the surrounding lipid matrix [11]. They are enriched in gel phase forming lipids like sphingolipids and cholesterol and have liquid-ordered (l_o) phase behavior. The properties of lipid rafts have been studied extensively in symmetric model membrane systems; however, biological membranes are asymmetric. Lipid rafts are localized on the outer leaflet of the plasma membrane, whereas phosphoinositides are localized on the inner leaflet of the plasma membrane. Recently, methodologies have emerged to fabricate asymmetric vesicles [12-14]. Studies with asymmetric vesicles have demonstrated that the phase behavior of one leaflet can exert influence on the phase behavior of the opposing leaflet. This interaction is called interleaflet coupling [13].

It has been hypothesized that lipid rafts may play a role in regulation of signaling at the membrane by an interleaflet coupling mechanism, illustrated in Figure 1. In this mechanism, a lipid raft domain in the outer leaflet induces formation of a domain in the inner leaflet, which presumably would also exhibit l_o phase type behavior. This inner leaflet l_o domains serves as a localized platform for signaling events to occur. It is believed that the l_o domain promotes clustering of certain proteins that prefer the l_o environment [15].

Based upon evidence of interactions between PI(4,5)P₂ and lipid rafts, it is hypothesized here that lipid raft domains in the outer leaflet induce the formation of a phosphoinositide-containing domain in the inner leaflet which serves as a signaling platform for phosphoinositide-mediated signaling. The acyl chain composition of PI(4,5)P₂ is not favorable for accumulation in a l_o environment. However, phosphoinositide domains can be formed in the presence of a stabilizing agent such as cholesterol [16] or calcium [17]. In order to investigate interleaflet coupling interactions between lipid rafts and phosphoinositide/cholesterol domains, asymmetric giant vesicles containing phosphoinositides are fabricated by the hemifusion method [14] and characterized by confocal microscopy.

2. Background

2.1 *Biological Membrane Structure*

In 1972, Singer and Nicolson proposed the fluid mosaic model of cell membrane structure. This model is still the basis of our understanding of membrane structure, although new experimental evidence has revealed additional layers of complexity beyond Singer and Nicolson's model. The fluid mosaic model posits that the membrane is composed of integral membrane proteins solvated in a dynamic, fluid phospholipid matrix, as illustrated in Figure 2. The phospholipid matrix is a bilayer in which the fatty acid chains are in contact with each other in the center and the polar head groups are exposed to the outside solvent. This formation of membrane structure is primarily driven by the thermodynamics of hydrophobic and hydrophilic interactions. Favorable interactions between the polar headgroups and aqueous environment are maximized, while the fatty acid chains are protected from contact with the aqueous environment, which minimizes the free energy of the structure [18].

Singer and Nicolson also stated that membranes are likely asymmetric [18]. Studies of erythrocyte membranes have revealed that each leaflet of the plasma membrane has a distinct phospholipid composition. The outer leaflet of the membrane is enriched in phosphatidylcholine (PC) and sphingolipids, while the inner leaflet is enriched in phosphatidylserine (PS), phosphatidylethanolamine (PE), and phosphatidylinositol (PI) [19, 20]. This asymmetry has important implications for both the structure and function of the membrane. Asymmetry contributes to curvature-induced mechanical stress in biomembranes, which is important for budding, fission, and fusion [20]. Loss of membrane asymmetry has downstream cellular consequences. For example, the presence of PS in the outer leaflet is associated with activation of apoptotic pathways and cell senescence. ATP-dependent flippase proteins facilitate the transport of a lipid from one leaflet to the other, and can either help maintain asymmetry or decrease it [21, 22].

More recent research has unearthed extensive evidence that biomembranes are also laterally asymmetric, although much debate remains on this topic. The idea of lateral asymmetry was first introduced with the discovery that epithelial cell membranes are polarized, in which the apical and basolateral domains of the membrane have distinct lipid composition [19, 23]. In 1997, Kai Simons and Elina Ikonen proposed a controversial theory: that membranes have lateral organization in the form of microdomains, or "rafts", that facilitate local accumulation of certain proteins and could act as platforms for signaling events to occur [11].

2.1.1 *Lipid Rafts*

The existence of lipid rafts has been a hotly debated topic since it was introduced in 1997. An abundance of evidence in support of lipid rafts has been uncovered over the past two decades, although raft models have changed considerably since first proposed. It is currently believed that lipid rafts are dynamic, nanometer-sized domains enriched in lipids with saturated acyl chains (sphingolipids) and cholesterol, as well as GPI-anchored proteins [19, 24, 25]. These lipid rafts domains form a more ordered, "liquid ordered" (l_o) phase, as opposed to the liquid disordered (l_d) phase of the surrounding unsaturated phospholipid matrix [26]. This lateral segregation of sphingolipids occurs presumably because of the preference of cholesterol's rigid,

planar sterol ring to interact with the stiffer, saturated acyl chains of sphingolipids over the bulkier, unsaturated acyl chains of most glycerophospholipids [24].

The coexistence of these domains can be directly observed in model membranes comprised of simple lipid mixtures, however, they have been difficult to observe in living cells [20, 27]. This challenge is likely due to the postulated nanometer-scale size of lipid rafts in physiological membranes, which is well below the optical resolution of visible light [24]. However, microscopic phase separation has been observed in giant plasma membrane vesicles (GPMVs), which contain the same diversity of lipids and proteins as cell membranes. Furthermore, lipids and proteins in GPMVs are sorted into the ordered and disordered phases according to the lipid raft hypothesis, providing convincing evidence that similar phase separation may occur in cellular membranes on a smaller scale [28].

New techniques designed to directly or indirectly observe lipid raft domains in GPMVs and living cells has provided further evidence that lipid rafts exist. Super-resolution light microscopy, FRET, and single-molecule tracking of designer fluorescent probes has been invaluable in these endeavors [28-30]. Direct visualization of liquid ordered domains in cells may soon be possible with a new technique that utilizes cryogenic electron microscopy to distinguish nanometer-sized liquid ordered domains in GPMVs [31]. These advances have led to the conclusion that lipid rafts more than likely play a role in physiological membranes; the implications of which are very exciting.

The potential functions of lipid rafts would provide a mechanism for spatial and temporal regulation of signaling events mediated at the plasma membrane [25]. With minimal energy expenditure, the cell could concentrate reactants of signaling pathways, exclude negative regulators, and regulate local membrane properties [28]. Simons & Ikonen proposed that proteins are selectively included or excluded from lipid rafts, providing a degree of lateral organization for protein functionality in the membrane. Additionally, lipid rafts are proposed to play a role in organization of membrane signaling, and important signaling lipids such as phosphatidylinositol-(4,5)-bisphosphate (PI(4,5)P₂) have been identified as potentially associated with lipid rafts [11].

2.1.2 Model Membranes

Model membranes have been utilized extensively for characterization of lipid phase separation and properties of lipid rafts. Model membranes are an ideal platform to characterize the phase behavior of various lipid mixtures due to their simplicity and the ability to tune the environmental surroundings of the membrane [32]. While studies conducted in model membranes will never show how complex biological membranes behave as a whole, they provide snapshots of the preferential behavior of certain lipids, which builds understanding of how lipids may interact in the plasma membrane. It is important to note that it is likely that integral proteins influence raft composition, size, and shape of lipid rafts in biomembranes [33]. Hence, model membranes cannot provide information about the influence of proteins on raft properties.

Types of model membranes include micelles, multilamellar vesicles, small unilamellar vesicles, large unilamellar vesicles, giant unilamellar vesicles, and supported lipid bilayers, which are illustrated in Figure 3. Model membranes have been particularly useful in determining

the formation and behavior of lipid raft domains. However, the vast majority of this research has been conducted using symmetric model membranes. As lipid raft domains have only been observed to form in outer leaflet lipid mixtures, it remains to be seen whether the formation of ordered lipid raft domains in the outer leaflet has an effect on the order of the inner leaflet or vice versa. Such an interaction is referred to as interleaflet coupling [13]. It is likely that lipid rafts exist in both the inner and outer leaflets, and that the properties of lipid rafts in the inner leaflet differ significantly from outer leaflet rafts due to differences in lipid composition [33]. Thus, symmetric model membranes have limited usefulness for investigating lipid rafts.

2.1.3 Asymmetric Model Membranes

In response to the need for asymmetric membrane models to investigate the potential effects of lipid rafts on both leaflets, multiple methods have been developed to create asymmetric model membranes [13, 14, 34-37]. The fabrication of asymmetric vesicles can be used to investigate effects of lipid raft domains on the phase behavior of both leaflets. In particular, giant unilamellar vesicles (GUVs), which are large enough to be observed under the microscope, can be used to directly observe domain formation in asymmetric vesicles. Two methods have been developed to form asymmetric GUVs (aGUVs). The first method, introduced in 2011, uses methyl- β -cyclodextrin (m β CD), a molecule that binds both cholesterol and phospholipids, to exchange lipids between heavy donor vesicles and symmetric GUVs, which are then separated from the donor vesicles once asymmetry has been achieved [13, 35]. The second method, published in 2019, utilizes hemifusion induced by calcium cations to fabricate aGUVs from symmetric GUVs and donor lipids in a supported lipid bilayer. Hemifusion is the fusion and mixing of lipids between the outer leaflet of two bilayers, excluding the inner leaflets [38]. This elegant method is illustrated in Figure 4 and creates aGUVs free of any contaminants such as organic solvents and cyclodextrin which are used in other aGUV methods [14].

2.2 Phosphoinositides and PI(4,5)P₂

Phosphoinositides are a class of phospholipids found in biological membranes that serve critical roles as regulators of a plethora of cell signaling pathways, including pathways that control cell communication, cell survival and proliferation, membrane trafficking and sorting, and gene expression, among others. As such, they are implicated in many disease states, such as cancer, diabetes, cardiovascular disease, and Alzheimer's. [1] Understanding the behavior and function of these molecules in biological membranes is imperative to understanding the regulation of these pathways.

Phosphoinositides are classified into groups of phosphorylated derivatives of phosphatidylinositol (PI), a glycerophospholipid with a myo-inositol ring as the head group, shown in Figure 5. Phosphorylation occurs at the 3, 4, and/or 5 positions of the inositol ring, leading to seven unique species of phosphoinositides (PIPs). Each PIP species plays different roles in signal transduction and have unique spatial distribution in the plasma and organelle membranes. [1] For example, PI(4)P is enriched in the golgi and is necessary for formation of secretory vesicles from the golgi [39].

Of particular interest among the phosphoinositides is PI(4,5)P₂, which is illustrated in the bottom of Figure 5. It is the most abundant phosphoinositide species in humans, accounting for

45% of all phosphoinositide species. Even though PI(4,5)P₂ is the most abundant phosphoinositide, it comprises only 1% of the total plasma membrane lipids, where it is primarily localized in the inner leaflet [40]. Yet for such a seemingly minor fraction of the plasma membrane, PI(4,5)P₂ is involved in the regulation of a surprising number of cellular processes, including cytoskeleton dynamics, clathrin-mediated endocytosis, exocytosis, phagocytosis and pathogen entry, calcium signaling, production of secondary messengers, enzyme activity, and more [39-42]. PI(4,5)P₂ is also found in the nuclear membrane where it is involved in the regulation of pre-mRNA splicing [39]. Signaling events mediated by PI(4,5)P₂ control downstream processes including cell movement, differentiation, and cell growth and proliferation [1, 40]. It is no wonder that PI(4,5)P₂ dysregulation has been linked to many diseases and disorders, such as Alzheimer's Disease, diabetes, cancers, and autism spectrum disorder. Characterizing the physiochemical properties of PI(4,5)P₂ and the mechanisms by which PI(4,5)P₂ signaling is regulated is integral to understanding signaling events mediated by PI(4,5)P₂ and the role of PI(4,5)P₂ in disease.

2.2.1 Lateral Organization of PI(4,5)P₂

Numerous studies have suggested that PI(4,5)P₂ forms microdomains in the plasma membrane [6, 8, 43-45], and several have linked these PI(4,5)P₂ microdomains to lipid raft domains [6, 43]. Laux et al. showed that GAP43, MARCKS, and CAP23, three proteins that affect actin cytoskeleton regulation, and PI(4,5)P₂ may colocalize at submicroscopic lipid microdomains. Additionally, they found that CAP23 is associated with lipid rafts domains in the plasma membrane [43]. These results suggest that PI(4,5)P₂ microdomains may potentially colocalize with lipid raft domains. Similarly, Furt et al. identified 25 nm microdomains of PI(4,5)P₂ clusters in the plasma membrane using electron microscopy. This study also found evidence that these microdomains may be linked to lipid rafts. An analysis of detergent resistant membranes of tobacco plasma membranes showed enrichment in polyphosphoinositides, suggesting that lipid rafts may play a role in the regulation of PI(4,5)P₂ signaling events [6].

But how does PI(4,5)P₂ cluster in these microdomains? The notion that PI(4,5)P₂ may form microdomains ubiquitously throughout plasma membranes, providing a mechanism for spatiotemporal control of PI(4,5)P₂ signaling events initially seems counterintuitive. The arachidonic acid residue of PI(4,5)P₂ does not favor partitioning into lipid rafts [44]. Additionally, the negative charge of the phosphorylated head group should repel neighboring PI(4,5)P₂ molecules, further disfavoring partitioning into stable domains. However, experimental evidence has shown that both cholesterol and divalent calcium ions can stabilize PI(4,5)P₂ interactions, leading to formation of stable domains. Jiang et al. showed that PI(4,5)P₂ forms stable domains in the presence of cholesterol. Cholesterol is proposed to act as a spacer between PI(4,5)P₂ molecules, reducing electrostatic repulsion between the phosphorylated headgroups, while the hydroxyl headgroup of cholesterol participates in a hydrogen bond network with PI(4,5)P₂ leading to stabilization [16]. Additionally, Wen et al. demonstrated that PI(4,5)P₂ clustering can be induced by divalent calcium ions [17], providing another mechanism by which PI(4,5)P₂ may be stabilized in microdomains.

2.2.3 *PI(4,5)P₂ Signaling Events are Linked to Lipid Rafts*

In addition to evidence that PI(4,5)P₂ microdomains may colocalize with lipid rafts, many studies have shown a link between PI(4,5)P₂-mediated signaling events and lipid rafts. Several studies have proposed this connection based on cholesterol dependence of signaling events as demonstrated by cholesterol-depletion studies [2-4, 7, 9]. However, as depletion of cholesterol affects not only lipid-raft mediated signaling, but also structure and fluidity of the membrane, these studies alone do not provide conclusive evidence of a link between lipid rafts and phosphoinositide signaling. Studies demonstrating colocalization of phosphoinositide binding domains and raft markers or raft-associated proteins have provided more compelling evidence of a link between PI(4,5)P₂-mediated signaling events and lipid rafts [5-8, 10].

2.2.4 *Coupling of Phosphoinositide Domains and Lipid Raft Domains*

Considering the evidence that PI(4,5)P₂ has been observed to form microdomains, that these microdomains may be spatially linked to lipid raft domains, and PI(4,5)P₂-mediated signaling events are linked to lipid rafts, it seems highly likely that some interaction between phosphoinositide domains and lipid raft domains modulates PI(4,5)P₂-mediated signaling events through spatiotemporal control. One potential regulation mechanism is interleaflet coupling, in which the lipid raft domains of the outer leaflet are in direct contact with phosphoinositide microdomains on the inner leaflet.

No study to date has characterized the conditions under which interleaflet coupling may occur or the properties of such an interaction, however theories exist that point to the plausibility of this interaction. It is theorized that organization of the outer leaflet into lipid rafts may induce phase separation in the inner leaflet [20]. Additionally, it is believed rafts exist in both leaflets of the bilayer, and that inner leaflet rafts are less stable than outer leaflet rafts due to the increased fraction of cis unsaturated acyl chains in the inner leaflet [33]. Coupling of an inner leaflet raft with a more stable outer leaflet raft may stabilize the formation of rafts in the inner leaflet. Studies in aGUVs have indeed shown evidence that interleaflet coupling can affect the physical state of both leaflets [13, 35], providing evidence that the outer leaflet rafts may have a stabilizing effect on their inner leaflet counterparts. In physiological cells, interleaflet coupling may be further stabilized by cellular components such as proteins and the cytoskeleton [33], however these interactions are beyond the scope of this thesis.

2.3 *Hypothesis*

The hypothesis investigated in this thesis is that interleaflet coupling occurs between phosphoinositide-cholesterol domains and lipid raft domains. To test this hypothesis, aGUVs containing phosphoinositides were fabricated using the hemifusion method [14]. An illustration of the experiment scheme is shown in Figure 6. When aGUVs are fabricated with a phase separated lipid raft mixture in one leaflet and PI(4,5)P₂ in the other, the question is which domain will the PI(4,5)P₂ lipids register with. The hypothesis says that a PI(4,5)P₂-cholesterol domain would register with the l_o phase of the lipid raft mixture. This interaction would provide proof of concept for a mechanism by which lipid rafts regulate phosphoinositide-mediated signaling events through interleaflet coupling. The fluorescence intensity of the aGUVs were analyzed to

assess the degree of asymmetry and quality of vesicles. Coupling of phosphoinositides and lipid raft domains was characterized using fluorescence probes and confocal microscopy.

3. Methodology

Materials

DOPC (1,2-dioleoyl-sn-glycero-3-phosphocholine), POPS (1-palmitoyl-2-oleoyl-sn-glycero-3-phospho-L-serine), DPPC (1,2-dipalmitoyl-sn-glycero-3-phosphocholine), brain PI(4,5)P₂ (L- α -phosphatidylinositol-4,5-bisphosphate), TopFluor PC (1-palmitoyl-2-(dipyrrometheneboron difluoride)undecanoyl-sn-glycero-3-phosphocholine), TopFluor TMR PI(4,5)P₂ (1-oleoyl-2-(6-((4,4-difluoro-1,3-dimethyl-5-(4-methoxyphenyl)-4-bora-3a,4a-diaza-s-indacene-2-propionyl)amino)hexanoyl)-sn-glycero-3-phosphoinositol-4,5-bisphosphate), and cholesterol were purchased from Avanti Polar Lipids (Alabaster, AL). Indium tin oxide coated cover slips (22x22 mm, thickness #1.5, 70-100 ohms resistivity) were purchased from SPI Supplies (West Chester, PA). Rhod-5N (tripotassium salt, cell impermeant) was purchased from Invitrogen (Carlsbad, CA). Lab-Tek II 4-well chambered coverglass was purchased from Thermo Fisher Scientific (Waltham, MA).

GUV Preparation in High Salt Buffer

Electroformation in physiological salt buffer was attempted under multiple conditions. This highest yield GUVs were prepared by electroformation in phosphate buffered saline as described by reference [46]. Indium tin oxide (ITO) coated slides were rinsed with isopropanol and dried in an oven at 60-70°C. 7 μ L of lipid mixture was spread evenly onto the ITO-coated surface of each slide using a 10 μ L microsyringe. The slides were dried for 5 minutes under N₂ gas. A 1.5 mm thick plastic spacer was sandwiched between the slides using a small amount of vacuum grease with the ITO/lipid side facing inward. Phosphate buffered saline (137 mM NaCl, 2.7 mM KCl, 8 mM Na₂HPO₄, 2 mM KH₂PO₄, pH 7.4) was injected into the electroformation chamber. The slides were attached to a function generator using conductive copper tape and alligator clips. An AC sine waveform was applied at 500 Hz. The peak-to-peak amplitude was increased from 0.65 V to 4.175 V over the course of 30 minutes, then 4.175 V was applied over an overnight swelling period of 14-20 hours. The frequency was decreased from 500 Hz to 50 Hz over a 30-minute period. Voltage and frequency was monitored using an oscilloscope throughout. Vesicles were stored at 4°C.

GUV Preparation in Sucrose (Low Salt) Buffer

GUVs were prepared by electroformation as described by [47]. ITO coated slides were prepared as described above. Sucrose buffer (200 mM sucrose, 1 mM NaCl, 1 mM HEPES, pH 7.4) was injected into the electroformation chamber. The slides were attached to an AC power supply (Hewlett-Packard 3311A Function Generator) using conductive copper tape and alligator clips.

For DOPC Vesicles:

Vesicles were electroformed at room temperature under conditions optimized for unsaturated lipid vesicles [48] with an 8 Hz AC sine wave. The peak-to-peak amplitude was set to 200 mV

initially and increased in a step-wise fashion by 100 mV every 5 minutes until the amplitude reached 1.25 V. Electroformation was continued at 1.25 V for 3 hours. To detach, a 4 Hz square waveform was applied for 1 hour. Voltage and frequency was monitored using an oscilloscope throughout. Vesicles were stored at 4°C for up to 3 days.

For DOPC/DPPC/Cholesterol Vesicles:

Prior to addition of buffer described above, the slides and buffer were preheated in an oven at 70°C. Vesicles were electroformed at 70°C with an AC sine wave at 10 Hz and 1.1 V peak-to-peak amplitude for 1 hour. After 1 hour, peak-to-peak amplitude was increased to 1.5 V for 2 hours. To detach vesicles, a 4 Hz square waveform was applied for 1 hour. Voltage and frequency was monitored using an oscilloscope throughout. Vesicles were slowly cooled to room temperature overnight and stored at 4°C for up to 3 days.

SUV Preparation

SUVs were prepared via sonication. Lipid mixture was dried under N₂ gas, placed in a vacuum oven for ≥ 2 hours, then rehydrated in 500 µL buffer A (25 mM HEPES pH 7.4, 35 mM KCl, 50 mM NaCl, 231 mOsm/kg) for a total lipid concentration of 2.5 mM. This lipid mixture was sonicated using a probe tip sonicator for 10 minutes at 30% amplitude with a 5 seconds on/off cycle, then centrifuged in a tabletop microcentrifuge for 20 minutes at 17,200 rcf to sediment titanium particles shed from the sonicator probe. Following centrifugation, vesicles were transferred to a fresh vial and vesicle size was confirmed using a Malvern Zetasizer. SUVs were diluted to 0.5 mM with 1 M NaCl. SUVs were stored at 4°C for up to 2 days.

LUV Preparation

LUVs were prepared via extrusion. Lipid mixture was dried under N₂ gas, placed in a vacuum oven for ≥ 2 hours, then rehydrated in 500 µL buffer A for a total lipid concentration of 2.5 mM. Vesicles were extruded 33X through a 100 nm pore membrane and size was confirmed using a Malvern Zetasizer. LUVs were diluted to 0.5 mM with 1 M NaCl and stored at 4°C for up to 1 week.

Supported Lipid Bilayer Preparation

Lab-Tek 4-well covered chamber glass slides were rinsed with a fresh preparation of 1 M KOH in ethanol, flushed with an abundance of ultrapure water, dried under N₂ gas, then subject to a plasma cleaner (Mercator Control Systems LF-5 Plasma System) with O₂ for 2 minutes. 500 µL of either SUVs or LUVs were added to chamber wells and let sit for 1 hour at room temperature to allow formation of a supported lipid bilayer (SLB). The SLB was washed by submerging in 2.5 L of ultrapure water and flushing each chamber with 20 mL of water using a syringe. The buffer in the chamber was replaced with buffer A while keeping the SLB hydrated. SLBs were stored at 4°C for up to 5 days.

Buffer Osmolality

The osmolality of all buffers used for the preparation of aGUVs was measured using osmometer model 5004 (Precision Systems, Natick, MA). Osmolality was measured in triplicate and adjusted to be within 3 units of 230 mOsm/kg using 1 M NaCl as necessary.

Asymmetric GUV Preparation by Hemifusion

Asymmetric GUVs were prepared by hemifusion as described by Thais Enoki and Gerald Feigenson [14]. Buffer in the SLB chamber was replaced by buffer B (25 mM HEPES pH 7.4, 35 mM KCl, 50 mM NaCl, 1 mM CaCl₂, 231 mOsm/kg) without dehydrating the SLB. 40-75 μ L GUVs were added to the SLB chamber in 5 μ L aliquots and were allowed to settle for 5 minutes. GUVs were imaged briefly before moving forward to confirm they had settled on the SLB surface. Calcium concentration was increased by adding 50-75X 5 μ L aliquots of buffer C (25 mM HEPES pH 7.4, 25 mM KCl, 20 mM CaCl₂, 40 mM NaCl, 232 mOsm/kg) to increase the calcium concentration to ~4-6 mM Ca²⁺. GUVs were incubated with SLB and calcium for 30 minutes, then imaged briefly to check extent of hemifusion. 1 mL buffer D (25 mM HEPES pH 7.4, 25 mM KCl, 20 mM EDTA, 40 mM NaCl, 232 mOsm/kg) was added to chelate calcium and stop hemifusion.

Determination of Calcium Concentration

The calcium-sensitive dye Rhod-5N was used to determine calcium concentration for the hemifusion experiments. A standard curve of calcium concentrations ranging from 0 (EDTA added) – 10 mM was created using CaCl₂ with 0.5 μ M Rhod-5N in a pH 7.4 HEPES buffer. Samples from the hemifusion experiments were taken out and diluted to a final volume of 2 mL. Rhod-5N was added to a final concentration of 0.5 μ M. The samples were measured in quartz cuvettes with a fluorimeter at 551 nm excitation. Emission was scanned over the range of 560-700 nm.

Confocal Imaging

Vesicles were imaged in the electroswell chamber or the SLB well using a Zeiss LSM 510 confocal microscope with a 63x oil DIC objective. Rhodamine-PE and TopFluor TMR PI(4,5)P₂ were excited with an argon laser at 543 nm with 40% power and 40% transmission. TopFluor PC and NBD-PS were excited with an argon laser at 40% power at 477 nm, 30% transmission and 488 nm, 40% transmission. Microscope settings were kept consistent for comparison of fluorescence intensity in symmetric and asymmetric GUVs. Zeiss software and ImageJ were used to analyze the images captured.

Fluorescence Recovery after Photobleaching (FRAP)

FRAP was performed with the same confocal microscope as described above. Three image frames were collected with normal laser intensity, then the SLB was bleached with maximum laser intensity for 3 frames within a circular ROI with radius 7 μ m. Following bleaching, 17 image frames were collected. Fluorescence intensity within the ROI was quantified using ImageJ software.

GUV Image Analysis

Fluorescence intensity analysis of GUVs was carried out in ImageJ as described by Thais Enoki and Gerald Feigenson [14]. Briefly, lines were drawn from the center of the GUV to the image frame. These lines were drawn at each degree around the circumference of the vesicle and fluorescence intensity was recorded for each point along the line. The maximum intensity,

corresponding to the bilayer of the GUV was determined. For phase separated GUVs, the fluorescence intensity of each phase was analyzed separately.

4. Results

4.1 Electroformation of GUVs can be carried out in low and high salt

In order to fabricate aGUVs, symmetric GUVs first needed to be prepared in high yield. The initial goal was to form GUVs in physiological salt concentration (~150 mM) in order to most closely mimic the physiological environment of a cell. However, formation of GUVs under high salt concentrations typically results in lower yields of vesicles than low salt. For this reason, GUV formation was also optimized under low salt conditions as well.

GUVs were prepared by electroformation, also referred to as electrosweeling [47]. When the electroformation method was initially introduced, it was thought that formation of vesicles under high salt was not possible using this method. While the exact mechanism by which salt hinders vesicle formation is unknown, it is theorized that the salt ions shield the lipid bilayers from the AC current, preventing swelling of the bilayers [49]. Phospholipids with charged head groups (such as phosphatidylserine - POPS) hinder the electroformation process even further when present in the lipid mixture because their charge contributes to the shielding effect. In the past decade, however, multiple groups have published methods for electroformation of giant vesicles under physiological salt concentrations [46, 49-52]. These methods report that increasing the frequency of the AC field 10-100-fold higher than the frequency typically used for electroformation under low salt (10 Hz) leads to successful formation of vesicles in a high salt environment. Li et al. was even able to form pure charged POPS vesicles in 150 mM salt using electroformation at high frequency [49].

To investigate the optimal conditions for electroforming vesicles under high salt, formation of pure DOPC vesicles in 100 mM NaCl or phosphate buffered saline (PBS) was attempted under a variety of conditions [49, 51, 52] as summarized in table 1. DOPC was chosen to test various methods because it is inexpensive and has a phase transition temperature well below room temperature, eliminating the need to swell at an elevated temperature. DOPC GUVs sized 10-20 μm in diameter were successfully swelled in PBS buffer as seen in Figure 7A, 7C, and 7D. Many factors affected the quality of vesicles formed. The best results were obtained by swelling on ITO coated slides in PBS at 500 Hz, as described by Lefrancois, Goudeau, and Arbault [46]. The voltage was increased from 0.65 V to 4.175 V over the course of 30 minutes, then 4.175 V were applied overnight. A long overnight step was required for vesicle formation. Overnight time periods ranging from 14-20 hours all resulted in successful vesicle formation, however decreasing this time period to 8 hours was not sufficient and resulted in clumps of multilamellar vesicles < 10 μm in diameter. High frequency was necessary to form vesicles in high salt buffer. Electroformation in high salt buffer has been reported at frequencies ranging from 300 Hz – 100 kHz [49]. Here, the best results were obtained at 500 Hz, however low yields of vesicles were also obtained at other frequencies reported in Table 1. Both ITO coated slides and platinum wires were tested as electrodes. The best yields were achieved by swelling on ITO coated slides; swelling on platinum wires resulted in either a low yield or no vesicles formed.

Vesicles formed by electroformation often stick to the electrode, and a detachment step is necessary to remove the vesicles from the slide surface. This was observed to be true for all preparations of electroswellable vesicles in this study. Vesicles still attached to the slide surface can be seen in Figure 7A and 7B. Detachment was attempted by repeated pipetting above the slide surface or by decreasing the frequency at the end of the electroswelling period. Decreasing the frequency was found to be the most efficient method, but the best results were frequently obtained by combining both these methods. However, both methods left a significant portion of vesicles attached to the slide. Detachment could be marginally improved by increasing the length of the low frequency treatment, without rupturing the vesicles.

After successful formation of DOPC GUVs in high salt, vesicles were formed with a mixture of 70% DOPC and 30% POPS to test the feasibility of electroforming GUVs with charged lipids in a high salt buffer. This lipid mixture was chosen to simulate the negative charge that would be introduced in a lipid mixture with 10-15% PI(4,5)P₂. Vesicles with 30% PS were formed successfully using the same conditions as the DOPC vesicles as seen in Figure 7B and 7E; however, a decreased yield was seen compared to the DOPC vesicles. These vesicles were also 10-20 μm in diameter, but their average diameter was smaller than the DOPC vesicles with a higher percentage of multilamellar or deformed vesicles.

Asymmetric GUV formation is not 100% efficient, so a high yield of GUV fabrication is needed to maximize overall yield. To this end, we tested whether a more efficient yield of GUVs could be obtained in low salt compared to high salt.

Electroformation in a low salt buffer is essentially the same as swelling in a high salt buffer, but the parameters for frequency, voltage, and duration of applied AC current are changed. Electroswelling of DOPC vesicles in low salt buffer (1 mM HEPES, pH 7.4, 1 mM NaCl, 200 mM sucrose) resulted in a high yield of vesicles 10-20 μm in diameter, as seen in Figure 8. Similar to the high salt protocol, this procedure comprised a step-wise increase in voltage, followed by AC current applied at peak voltage, and then a frequency decrease to detach [48]. Each of these parameters were decreased compared to those used for the high salt vesicles. High frequency is unfavorable for swelling in low salt and the voltage and swelling period was decreased accordingly as well.

One large difference observed between the low salt and high salt GUVs is that detachment by decreasing the frequency was more efficient for the low salt GUVs. This factor contributed to the increased overall yield of GUVs in low salt. Greater detachment efficiency resulted in a higher proportion of GUVs in solution that could be removed from the swelling chamber for aGUV fabrication.

It was decided to first optimize aGUV formation using the GUVs swollen in low salt because they had a higher effective yield. To this end, GUVs with a lipid raft mixture were swollen in low salt buffer. The lipid raft mixture was composed of 40% DOPC, 40% DPPC, and 20% cholesterol. This mixture is designed to phase separate into the l_d and l_o phases, mimicking the coexistence of liquid disordered and lipid raft domains in a cell membrane, but on a larger scale for ease of observation. The DOPC comprises the majority of the l_d phase, and the DPPC and cholesterol comprise the majority of the l_o phase, which mimics the properties of lipid rafts. The fluorescent probe included in the mixture was 0.05% TopFluor PC (TFPC), which is labeled with a BODIPY (boron-dipyrromethene) group on the end of one of the acyl chains. TFPC

preferentially partitions into the l_d phase because the bulky BODIPY group on the acyl chain is not amenable to the close packed environment of the l_o phase. In Figure 9A, the coexistence of these domains in the phase-separated GUVs can be clearly seen, with the brighter fluorescent portion of each vesicle representing the l_d phase as the fluorescent TFPC lipid is more concentrated in this region of the bilayer. These lipid raft GUVs formed in similar yield to the DOPC GUVs in low salt buffer.

4.2 Fluorescence recovery after photobleaching confirms supported lipid bilayer formation

Supported lipid bilayers (SLBs) were fabricated from either SUVs or LUVs. The SLBs serve as donor lipids for the hemifusion process. The lipid mixture in the SLB will become the outer leaflet of the aGUVs. For optimization of aGUV formation by hemifusion, SLBs composed of 80% DOPC, 20% POPS, and either 0.2% rhodamine-PE or 0.2% NBD-PS were fabricated. The POPS was intended to simulate the negative charge of 10% PI(4,5)P₂ during the initial troubleshooting of the hemifusion process. For experiments with PI(4,5)P₂ aGUVs, a SLB composed of 90% DOPC, 10% PI(4,5)P₂ and 0.1% TopFluor TMR PI(4,5)P₂ (TFTMR PIP₂) was fabricated.

Fluorescence recovery after photobleaching was used as a spot check to ensure the SLB had successfully formed. The SLBs fabricated from SUVs exhibited recovery of fluorescence over an area of approximately 154 μm subjected to photobleaching within 30 seconds, indicating that the lipids in the SLB are mobile and fluid. Example FRAP data from one SLB is shown in Figure 10. SLBs formed from LUVs also showed fluorescence recovery, but at a slower rate. A fluid SLB is necessary in order for hemifusion to occur. The formation of aGUVs was tested using both types of SLBs – originating from SUVs or LUVs.

4.3 Hemifusion is a viable method to form phosphoinositide-containing aGUVs

Asymmetric GUVs were prepared by hemifusion [14], using a SLB and symmetric GUVs. The symmetric GUVs were prepared by electroformation in low salt buffer as described in section 4.1. To confirm reproducibility of the procedure, aGUVs with a simple lipid mixture were fabricated. The symmetric GUVs, which became the inner leaflet of the aGUVs were composed of DOPC and 0.05% TopFluor PC or 0.2% Rhodamine-PE. The SLB, which became the outer leaflet of the aGUV was composed of 80% DOPC, 20% POPS, and 0.2% Rhodamine-PE or 0.2% NBD-PS. The inclusion of POPS in the outer leaflet was meant to simulate the negative charge introduced by PI(4,5)P₂. Hemifusion was first optimized for negatively charged outer leaflet phospholipids with this mixture, before incorporating PI(4,5)P₂.

Asymmetric GUVs with NBD-PS as the fluorescently tagged lipid in the outer leaflet were used to confirm that the elevated calcium concentration in the hemifusion process did not significantly or permanently cluster negatively charged lipids. Divalent cations such as calcium can bind to PI(4,5)P₂ molecules, inducing clusters. This interaction may alter interleaflet coupling interactions. Clustering would manifest as bright spots along the lipid bilayer, which would represent localized areas where the NBD-PS markers are more concentrated. No detectable clustering of POPS molecules was seen in the presence of calcium during hemifusion, or after EDTA was added, which was a promising sign that the same would be true of an experiment incorporating PI(4,5)P₂ into the outer leaflet.

Following successful fabrications of aGUVs containing POPS, aGUVs with an inner leaflet composition of DOPC with 0.05% TopFluor PC and an outerleaflet composition of 90% DOPC, 10% PI(4,5)P₂, and 0.1% TopFluor TMR PI(4,5)P₂ were fabricated. This experiment confirmed that hemifusion was compatible with PI(4,5)P₂ lipids in the supported lipid bilayer. The use of a fluorescently tagged PI(4,5)P₂ allowed investigation of calcium clustering. As seen with the POPS aGUVs, no visible clusters of PI(4,5)P₂ were observed. While full hemifusion and 100% asymmetry was not reached with these aGUVs, this experiment indicated that it was worthwhile to move forward with fabrication of lipid raft/phosphoinositide aGUVs.

Phosphoinositide-containing aGUVs were fabricated with lipid raft mixture GUVs swelled in low salt buffer and the same outer leaflet composition as described above. Hemifusion was observed by the appearance of the red TFTMR PIP₂ fluorophore in the vesicles, demonstrating that fusion had occurred. Hemifusion progress was monitored by observing the resulting vesicles by confocal microscopy, and EDTA was added when it appeared that TFPC and TFTMR PIP₂ had reached an approximately equal level of intensity. Both phase separated and non-phase separated aGUVs were observed. A phase separated aGUV is shown in Figure 12 and a non-phase separated aGUV is shown in Figure 11. The lipid raft mixture should phase separate if the ratios of lipids are true to the original composition. Therefore, it was assumed that the non-phase separated aGUVs had an altered lipid composition in the inner leaflet. The potential mechanisms that caused these non-phase separated GUVs to form will be discussed in detail later.

To quantify and analyze the degree of asymmetry reached, fluorescence intensity analysis was carried out using ImageJ. The lipid raft/phosphoinositide vesicles were separated into two populations—one non-phase separated and one phase separated. The non-phase separated GUVs were used for fluorescence intensity analysis, but not for observation of interleaflet coupling. It was easier to analyze fluorescence intensity for non-phase separated GUVs because the fluorescence is uniform through the bilayer. For this reason, analysis of these GUVs gave a clearer picture of the extent of asymmetry than the phase separated GUVs. As seen on the right in Figure 11, the intensity of TFPC decreases during hemifusion, while the intensity of the TFTMR PIP₂ increases during hemifusion. This clearly demonstrates that hemifusion has occurred and close to 100% asymmetry has been reached. The fluorescence intensity of TFTMR PIP₂ displays a significant increase, indicating that the SLB lipids did indeed fuse with the symmetric GUVs. The fluorescence intensity of each fluorophore is within the same level of magnitude and could be equal within the margin of error.

The phase-separated aGUVs exhibited phase separation in both leaflets. In the inner leaflet, phase separation was visualized using the selective partitioning behavior of TFPC. The outer phosphoinositide-containing leaflet uses the fluorescent PIP(4,5)P₂ analogue TFTMR PIP₂ to report the location of the PI(4,5)P₂ lipids. This fluorescent marker exclusively registered with the l_d domain of the inner leaflet as seen in Figure 12.

Like the non-phase separated aGUVs, the phase separated aGUVs displayed a clear increase in the fluorescence intensity of TFTMR PIP₂. However, this observation was only true for the l_d domain of the membrane. The l_o phase did not have any increase in fluorescence intensity for TFTMR PIP₂, as shown on the bottom of Figure 12. Interestingly, there was no

significant decrease in fluorescence intensity of TFPC after hemifusion in either the l_d or l_o domains. This observation will be further explored in the discussion section.

4.4 Calcium concentration

In order to confirm that all leftover calcium was chelated by EDTA following hemifusion, a calcium standard curve was prepared using the calcium sensitive dye Rhod-5N. This dye is sensitive to calcium concentration in the range of 0.1-10 mM. Rhod-5N has a λ_{max} of 572 nm, as seen in the top of Figure 13. Fluorescence emission intensity at 572 nm was plotted versus concentration as seen in the bottom of Figure 13. The fluorescence emission intensity at 572 nm of samples from four aGUV hemifusion experiments after EDTA addition was measured to determine the effectiveness of calcium chelation by EDTA. The fluorescence intensity for these samples fell in the range of 3.60 – 48.56, which is well below the fluorescence intensity of 0.2 mM calcium, which was the lowest concentration of calcium greater than 0 in the standard curve. Fluorescence intensity of the 0.2 mM calcium was measured at 425.7 ± 25.46 . These values suggest that the calcium concentration after EDTA addition is less than 0.1 mM, the sensitivity threshold of the dye.

5. Discussion

5.1 Symmetric GUV formation

GUVs were successfully formed in both low and high salt. Due to time constraints, the low salt GUVs were used to move forward with optimization of asymmetric GUV formation. However, high salt GUVs were also formed in adequate yield, which presents a future opportunity to fabricate asymmetric GUVs with a physiological salt environment on both sides of the membrane.

The best yields of high salt GUVs were achieved by swelling on ITO coated slides, however, many papers have reported good results when swelling on platinum wires [46, 51, 52]. Platinum wire is often considered a more advantageous swelling substrate for GUVs in high salt buffer because they are reusable and can tolerate higher currents as opposed to ITO slides. The ITO coating on slides will oxidize under high currents, and deteriorate over time. Once the ITO coating is oxidized, it will no longer produce good quality vesicles [52]. Despite this challenge, ITO slides have significant advantages. The slides have a higher surface area than platinum wires and therefore have the potential to produce a higher yield of vesicles. Additionally, ITO slides have the added advantage that vesicles can be imaged directly on the slides without needing to transfer to another chamber. The results reported here demonstrate that ITO coated slides are equally advantageous as platinum wires when electroswelling in high salt buffer, in line with results reported by others [46, 49].

It was observed that the GUVs swelled in low salt solution detached from the ITO coated slides more readily than the GUVs swelled in high salt solution. This factor contributed to the higher yield of low salt GUVs. The most effective detachment method was a decrease of frequency at the end of the swelling period. During electroformation, lipids follow the alternating changes in the electric field [52]. Decreasing the frequency slows down the changes in the electric field. The vesicles follow this slow field and are driven further away from the surface of the electrode under the decreased frequency, resulting in detachment and free-floating GUVs. In

a high salt buffer, this effect is minimized because the high concentration of ions help shield the lipids from the applied electric field [52]. GUVs swelled in high salt are inherently less prone to detachment, which means they are more difficult to work with when the GUVs need to be removed from the swelling chamber.

Future experiments should attempt aGUV formation using GUVs swelled in high salt. As these GUVs were found to form in lower yield, it will more challenging, albeit not impossible to transform them into aGUVs. With optimization and mastery of aGUV formation, successful fabrication using a lower yield of GUVs should be achievable. With a physiological salt concentration present on both sides of the membrane instead of just one, this aGUV system will more faithfully mimic the conditions of biological plasma membranes.

5.2 Differences between SLBs formed from SUVs and LUVs

Supported lipid bilayers were formed from either small unilamellar vesicles (SUVs) or large unilamellar vesicles (LUVs). It is more common to fabricate SLBs using SUVs. LUVs were used to fabricate SLBs because of concerns about the location of PI(4,5)P₂ in SLBs originating from SUVs. SUVs are smaller than LUVs, which gives the membrane more curvature. This high curvature may cause the PI(4,5)P₂ lipids to primarily localize to the outer leaflet of the SUV because there is less curvature stress in the outer leaflet. If the majority of the PI(4,5)P₂ is located on the outside of the SUVs, they will be mainly located in the bottom leaflet of the SLB, closest to the glass, where they will not participate in hemifusion or be incorporated into aGUVs. It was hypothesized that the SLBs formed from LUVs would result in better aGUV formation despite their slower fluorescence recovery.

No significant differences were seen between the aGUVs formed from SLBs originating from SUVs or LUVs. However, this observation is only based on observation of one experiment. It may be worthwhile to further explore and quantify if differences do indeed exist between the different SLB preparations, in regards to PI(4,5)P₂ localization. The aGUVs for which fluorescence intensity data is reported were fabricated using an SLB formed from LUVs.

5.3 Phase separated versus non-phase separated vesicles

Asymmetric GUVs with a lipid raft mixture inner leaflet and phosphoinositide-containing outer leaflet were successfully fabricated. However, this preparation of aGUVs resulted in both phase separated and non-phase separated aGUVs, as seen in Figures 12 and 11, respectively. Symmetric non-phase separated lipid raft GUVs can be seen in Figure 9B. This observation suggests that the lipid composition in these GUVs has been altered, as the 40% DOPC/40% DPPC/20% cholesterol mixture is expected to phase separate. Two explanations for this occurrence is offered.

When the symmetric GUVs are electroswelled, a lipid mixture in the desired ratio is dissolved in chloroform, then spread onto the ITO glass slides and dried. While every effort is made to ensure the lipids are distributed evenly (i.e. the lipid mixture is vortexed immediately before being applied to the ITO slide), small areas of non-uniform composition may still form within the dried lipid bilayers, where the lipid ratios are significantly altered from the overall ratio. It has been reported that heterogeneity can occur in GUVs from the same preparations [53]. GUVs that swell from these areas of bilayer will therefore have an altered lipid composition from the overall population. Furthermore, when the electroformation method is used, some types

of lipids may react to the electric field differently than others and be incorporated into the vesicles at different proportions [52]. Some of the non-phase separated GUVs observed may originate from heterogeneities during vesicle formation.

An alternative explanation is that the l_d phase in a phase-separated vesicle may have pinched off from the parent vesicle. This has been reported to happen in phase-separated vesicles during long cooling periods, especially if they have been formed by electroformation [54]. Additionally, pinching off has been observed to occur in phosphoinositide/cholesterol vesicles. The lipid raft mixture GUVs are swelled at an elevated temperature of 70°C, above the phase-transition temperature of DPPC, then cooled overnight, and stored at 4°C. It is very plausible that the l_d phase may have budded off from the l_o phase during the cooling period or during storage. GUVs were often stored for several days before use as they are generally stable for up to a week, which would have allowed ample time for budding to occur. Formation of non-phase separated vesicles may be minimized if GUVs are used soon after swelling.

The hypothesis that some of the non-phase separated GUVs may have pinched off from phase separated GUVs is supported by the observation that some of the non-phase separated GUVs varied significantly in the brightness of the fluorophore. Brighter GUVs may represent a l_d domain that pinched off from the phase separated vesicles, while dim GUVs would represent the l_o domain because TFPC is preferentially excluded from this phase. Some of the solely l_o phase GUVs may have even been too dim to visually observe. Furthermore, the proportion of non-phase separated GUVs seemed to increase after 24-48 hours of storage, further supporting this hypothesis.

5.4 Characteristics of phosphoinositide-containing aGUVs

Fabrication of asymmetric phosphoinositide-containing GUVs by hemifusion was demonstrated for the first time. Vesicle asymmetry was confirmed by fluorescence intensity. The fluorescence intensity data of the non-phase separated aGUVs demonstrated that near 100% asymmetry was achieved. In a perfect, 100% asymmetric vesicle, the TFPC is expected to decrease by 50%. However, in Figure 11 it decreases by more than 50%. One possible explanation for this observation is that the amount of TFPC was not completely uniform among the populations of vesicles measured before and after hemifusion. The before data was taken from a different preparation of GUVs than those used for the after data. While the two preparations were prepared in the same manner, opportunities for error exist. For example, if the amount of fluorescent lipid added to each of these preparations differed by even a fraction of a microliter, this could affect the fluorescence intensity of the vesicles.

An alternative explanation is that more than 50% fusion occurred. Full fusion may occur if the vesicles and SLB are incubated with calcium for too long. When more than 50% fusion occurs, the SLB lipids will begin to fuse with the inner leaflet, decreasing the percentage of asymmetry in the vesicle. Full fusion is undesirable because the goal is to form vesicles with near 100% asymmetry. To determine whether full fusion may have occurred under the conditions used to fabricate the aGUVs, several hemifusion experiments could be set up with EDTA added to stop the hemifusion at a range of time points. The degree of asymmetry should increase until the optimal hemifusion time is reached. Beyond this time point, the degree of asymmetry will begin to decrease.

The fluorescence intensity data of the phase separated aGUVs told a different story than the non-phased separated population. The fluorescence intensity of the TFFC fluorophore did not appear to decrease in either the l_d or l_o phases. Again, the before and after data was taken from different preparations of GUVs, so some of the error may originate in slight differences between the two GUV preparations. Additionally, the after data had quite a small sample size ($n=5$), which may be another source of error. This experiment should be repeated with a larger sample size, and the before and after data should be taken from the same population of GUVs to minimize error and confirm asymmetry of the vesicles.

Despite these discrepancies, the l_d phase shows a clear increase in the fluorescence intensity of TFFC. While it is unclear if these aGUVs had near 100% asymmetry, this observation demonstrates that significant transfer of TFFC did occur between the SLB and GUVs, indicating that some degree of asymmetry was reached. Although the sample size of phase-separated aGUVs was small, all of them showed exclusive registration between TFFC and the l_d domain in the opposing leaflet. This suggests that PI(4,5)P₂ has a preference for registration with the l_d domain under these conditions. Considering the small sample size and inconsistencies in this data, this experiment should be repeated to confirm this finding.

The calcium assay demonstrated that the calcium concentration present in the SLB chamber after hemifusion was very low—less than 0.1 mM. The EDTA step is especially important when PI(4,5)P₂ is present on the outside of the vesicle because calcium ions can bind to PI(4,5)P₂ molecules and cause clustering [17]. In the case of aGUVs fabricated with PI(4,5)P₂ on the outside, the possibility that some calcium may remain bound to the PI(4,5)P₂ headgroups as opposed to the EDTA was considered. However, this scenario is unlikely. EDTA is a polydentate ligand with a high affinity for bivalent cations such as calcium. The binding constant of this interaction is in the range of 10^8 [55]. A direct comparison to PI(4,5)P₂ is not possible because the binding constant for an interaction between calcium and PI(4,5)P₂ has not been measured. The affinity of PI(4,5)P₂ for calcium can vary due to many factors including the surrounding lipid composition and the curvature of the bilayer [56, 57]. However, it is unlikely that the affinity of PI(4,5)P₂ for calcium would be able to outcompete EDTA.

This work establishes phosphoinositide-containing asymmetric vesicles as an *in vitro* system in which the coupling of PI(4,5)P₂ and lipid rafts can be investigated. The formation of aGUVs containing phosphoinositide-containing vesicles serves as a proof of concept that interleaflet coupling of phosphoinositide-cholesterol domains can be investigated in an *in vitro* system. Additionally, this work opens many avenues for future exploration.

5.5 Future directions

Due to the closing of the WPI laboratories in response to the COVID pandemic, the experiments planned for this project were cut short, and a complete answer to the hypothesis was not found. It was observed that PI(4,5)P₂ had a preference for registration with the l_d domain of the opposing leaflet, but registration between PI(4,5)P₂ and lipid raft domains was only tested under one condition. The following experiments should be carried out in order to more fully characterize this interaction.

First, registration between PI(4,5)P₂ and lipid raft domains should be tested in the presence of cholesterol in the phosphoinositide leaflet. Cholesterol has been shown to stabilize phosphoinositide domains [16], and may potentially promote an interaction between PI(4,5)P₂

and l_o domains. Secondly, phosphoinositide/lipid raft interactions should be studied in the presence of calcium. Calcium is also known to promote and stabilize clustering of PI(4,5)P₂ in the membrane, and may therefore have a similar effect as cholesterol. If elevated calcium concentrations were able to promote an interleaflet coupling interaction between phosphoinositides and lipid rafts, this could have particular significance for calcium signaling [58].

Additionally, it should be confirmed that the phase partitioning behavior of TFTMR PIP₂ is the same as PI(4,5)P₂. Since TFTMR PIP₂ is being used as a reporter molecule for the location of PI(4,5)P₂, its accuracy needs to be validated. Validation of the location of PI(4,5)P₂ could be investigated by incubating the aGUVs with a fluorescent PI(4,5)P₂ binding partner and observing whether they display the same localization patterns as TFTMR PIP₂. Multiple fluorescent binding markers have been used to investigate PI(4,5)P₂ incorporation into membranes, including fluorescent PI(4,5)P₂ antibodies [59], the PH domain of phospholipase C labeled with Alexa 488, or GFP-conjugated septin proteins [60]. ζ -potential measurements [59] could also be taken to validate the incorporation of PI(4,5)P₂ into the outer leaflet, although this will not provide information about phase-partitioning behavior.

In the aGUVs that were fabricated, phosphoinositides are located on the outer leaflet while the lipid raft mixture is located on the inner leaflet, which is opposite to their locations in a biological membrane. Flipping this configuration in aGUVs has distinct advantages. By placing the phosphoinositides on the outer leaflet, they are exposed to the outer solution, which allows for manipulation with ions or molecules that bind to PI(4,5)P₂, such as calcium and fluorescent binding partners. Furthermore, it is much simpler to electroswell uncharged GUVs and place the negatively charged PI(4,5)P₂ molecules in the SLB.

Changing the configuration of the leaflets in the aGUVs to have phosphoinositides in the inner leaflet and the lipid rafts in the outer leaflet as in a plasma membrane presents opportunities to validate various concepts. Confining phosphoinositides to the inner leaflet of the aGUV will reveal if the presence of calcium has a lasting effect on phosphoinositide clustering, even after EDTA is removed. Additionally, the asymmetry of these vesicles could be confirmed by incubating with fluorescent PI(4,5)P₂ binding partners, to determine whether any PI(4,5)P₂ is still present in the outer membrane after hemifusion. Such an experiment could also determine loss of asymmetry over time by quantifying flip-flop of PI(4,5)P₂ from the inner to outer leaflet. A great advantage of working with aGUVs as opposed to biological membranes is that the composition of the inner and outer leaflets can be manipulated easily. Placing phosphoinositides in either the inner or outer leaflet both present unique opportunities to manipulate and characterize the asymmetric vesicles.

6. Conclusion

In conclusion, parameters were optimized for electroformation of GUVs in a physiological salt buffer with high yield. This work provides the opportunity to fabricate aGUVs with physiological salt concentrations on both sides of the membrane, creating a simplistic, biomimetic plasma membrane model. This advancement would increase the relevancy of this *in vitro* vesicle system towards making predictions about properties of the plasma membrane.

Furthermore, this project established a phosphoinositide/lipid raft asymmetric vesicle system which can be used to investigate interleaflet coupling interactions. This achievement lays the groundwork for investigating interleaflet coupling as a regulation mechanism of phosphoinositide-mediated signaling. Future work has been proposed to further characterize and validate the assumed properties of this system. Future experiments using this system have the potential to prove the concept for an interleaflet coupling regulation mechanism. These findings will have wide implications for many signaling pathways, including those that are implicated in disease states such as diabetes, cardiovascular disease, Alzheimer's disease, and cancer.

Tables and Figures

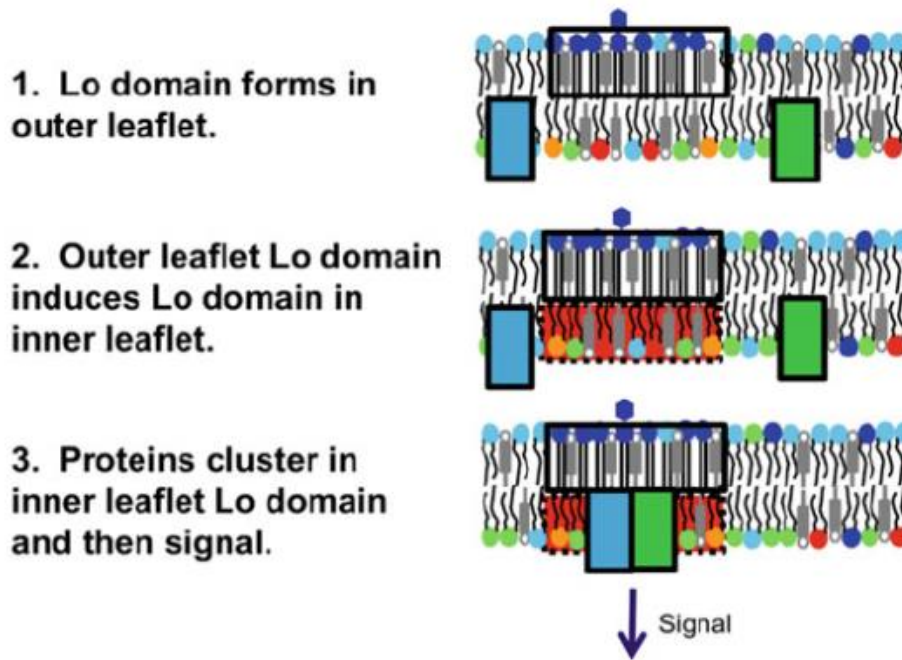


Figure 1. Proposed interleaflet coupling regulation mechanism of membrane signal transduction. Figure borrowed from ref [15].

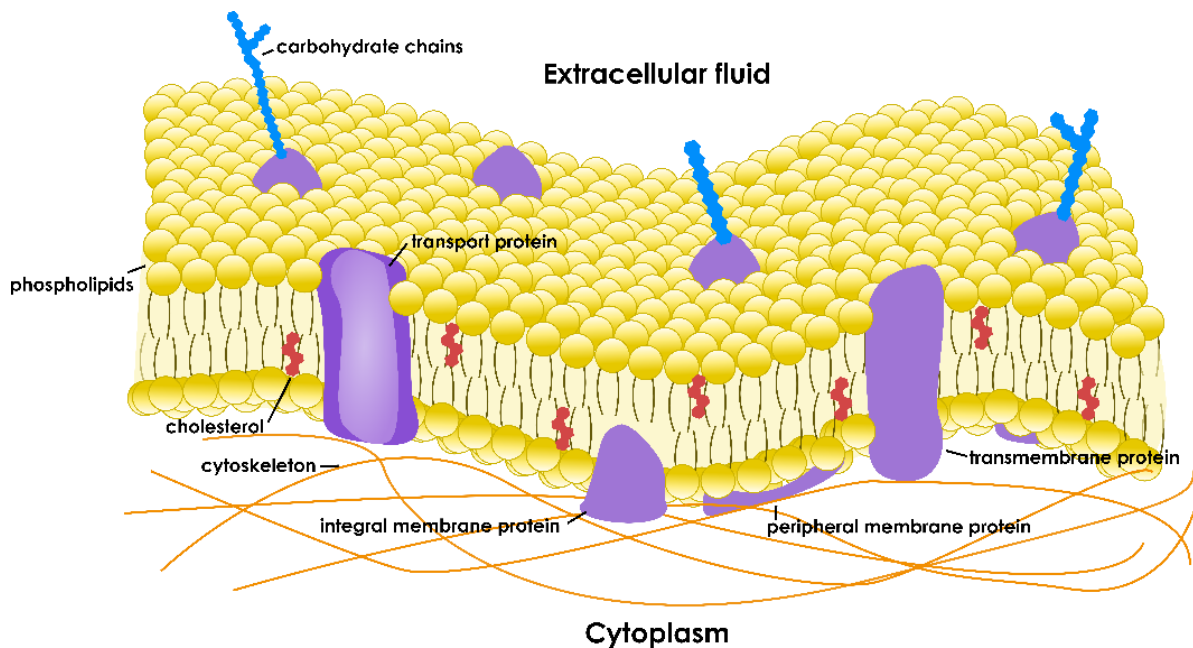


Figure 2. An illustration of the fluid mosaic model, proposed by Nicolson and Singer 1972. Integral membrane proteins are solvated in a matrix of phospholipids and cholesterol. Peripheral membrane proteins are attached by electrostatic forces and can be removed without compromising the structure of the membrane.

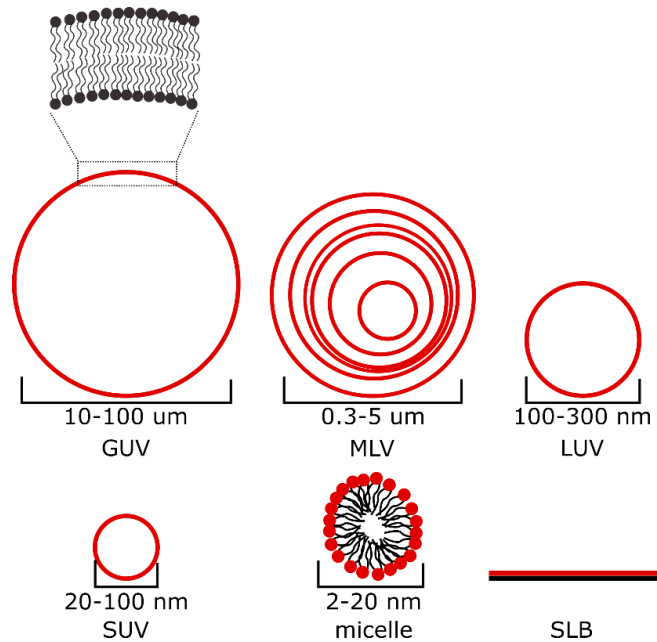


Figure 3. Diagram of model membrane types. Giant unilamellar vesicles (GUVs), large unilamellar vesicles (LUVs), and small unilamellar vesicles (SUVs) are all composed of a single bilayer, as opposed to multilamellar vesicles (MLVs), which have multiple bilayers. Micelles are not a bilayer, and instead have a spherical formation of lipids in which the fatty acid chains are in the middle with the polar head groups facing outwards towards aqueous solvent. A supported lipid bilayer is a single bilayer on top of a support, such as a glass slide. In this diagram, a single red line indicates a lipid bilayer.

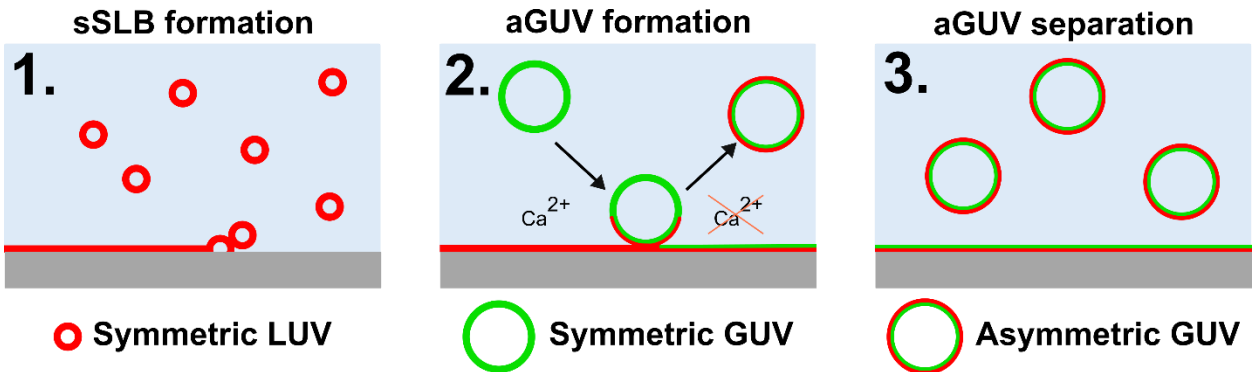


Figure 4. Formation of aGUVs by the hemifusion method. 1) Symmetric LUVs with the intended outer leaflet composition are deposited on a glass slide to form a supported lipid bilayer (SLB). 2) Symmetric GUVs with the intended inner leaflet composition are exposed to the SLB and calcium is added to initiate hemifusion between the GUVs and the SLB. EDTA is added to halt hemifusion. 3) aGUVs are separated from the SLB by gentle aspiration. The vesicles are now asymmetric, the outer leaflet having been replaced by lipids from the SLB.

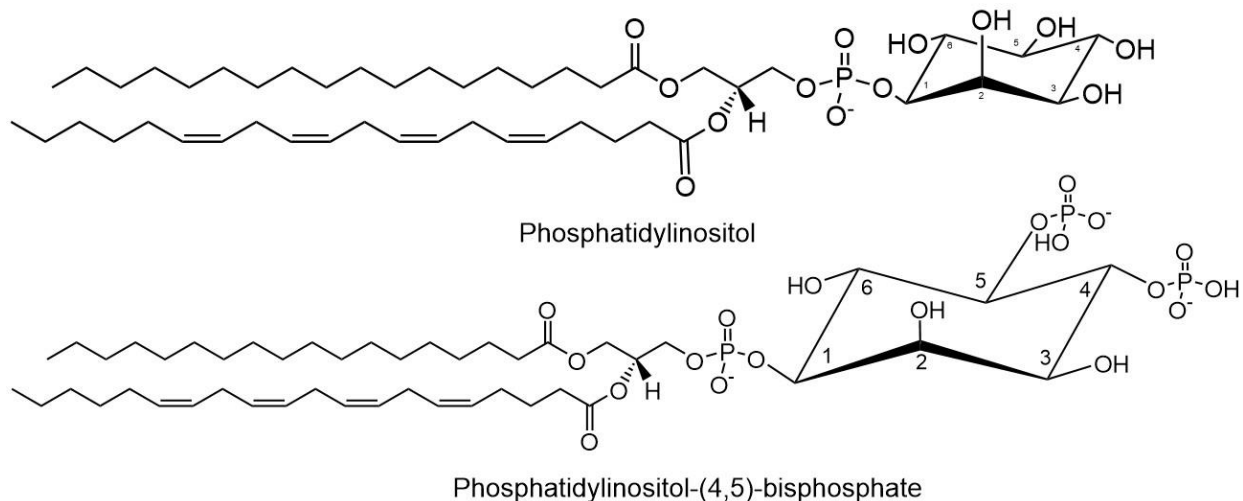


Figure 5. Phosphoinositide structures. **Top:** Structure of phosphatidylinositol, which can be phosphorylated at the 3,4, and/or 5 positions of the inositol ring to form polyphosphoinositides. **Bottom:** Structure of phosphatidylinositol-(4,5)-bisphosphate, which is phosphorylated on the 4th and 5th carbons of the inositol ring.

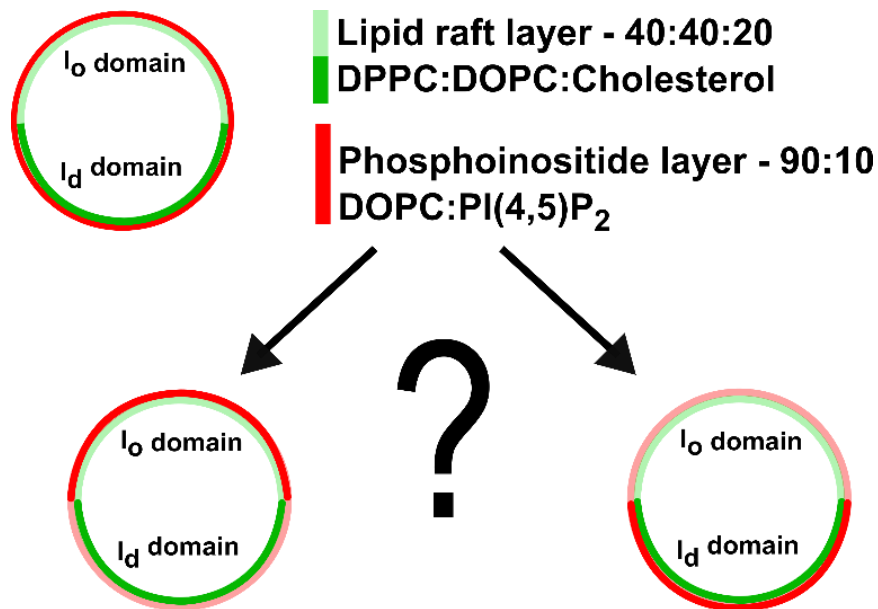


Figure 6. Graphical Hypothesis. In this experiment, an aGUV is fabricated with a phase separated lipid raft mixture in the inner leaflet, illustrated in green, and a phosphoinositide-containing outer leaflet, illustrated in red. The dark green represents the liquid disordered domain and the light green represents the liquid ordered domain. Dark red represents the area where phosphoinositides are most concentrated. The question is which domain will the phosphoinositides register with? According to the hypothesis, when the phosphoinositide leaflet contains cholesterol, the phosphoinositides will register with the liquid ordered domain

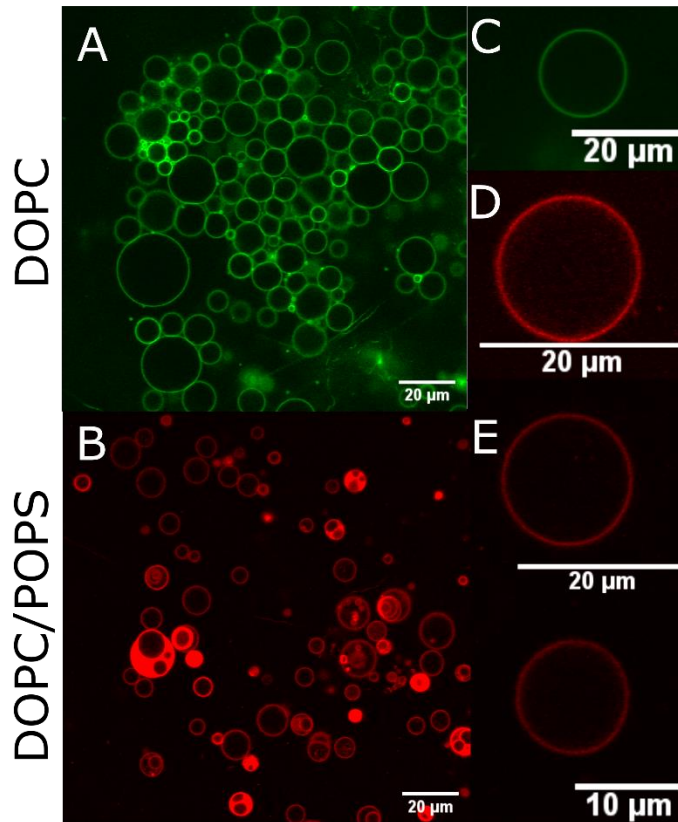


Figure 7. Vesicles formed by electroformation in PBS. **A:** DOPC vesicles with 0.2% TopFluor PC attached to ITO slide surface; **B:** 70% DOPC 30% POPS vesicles with 0.2% rhodamine-PE attached to ITO slide surface; **C:** DOPC vesicle with 0.2% TopFluor PC free floating in solution; **D:** DOPC vesicle with 0.2% rhodamine-PE free floating in solution; **E:** 70% DOPC 30% POPS vesicles with 0.2% rhodamine-PE free floating in solution

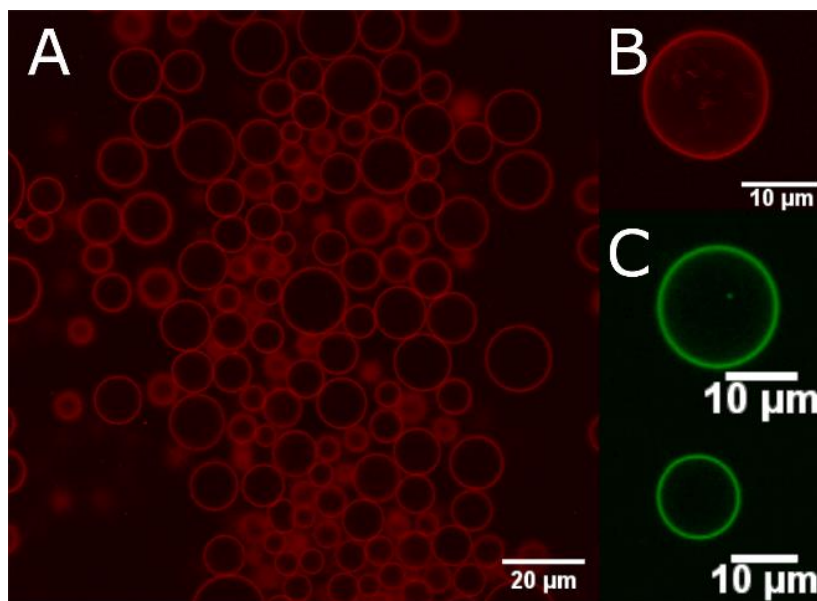


Figure 8. DOPC vesicles electroswelled in low salt buffer (200 mM sucrose, 1 mM HEPES pH 7.4, 1 mM NaCl). **A:** DOPC vesicles with 0.2% rhodamine-PE still attached to the ITO glass slide; **B:** free floating DOPC vesicle with 0.2% rhodamine-PE; **C:** free floating DOPC vesicles with 0.05% TopFluor PC.

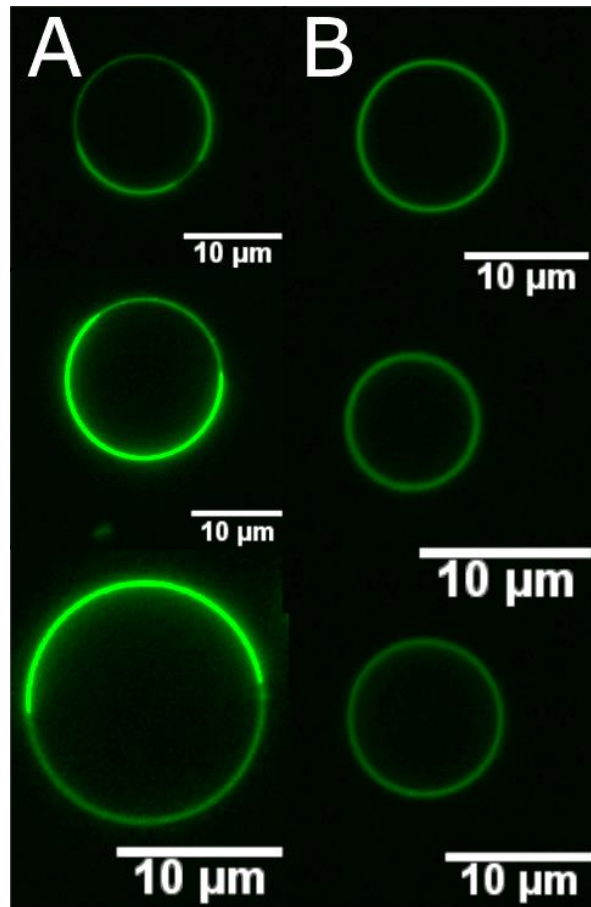


Figure 9. Lipid raft mixture GUVs swelled in low salt buffer. 40% DOPC 40% DPPC 20% cholesterol with 0.05% TopFluor PC vesicles electroswelled in low salt buffer (200 mM sucrose, 1 mM HEPES pH 7.4, 1 mM NaCl). **A:** phase separated GUVs. The bright regions correspond to the l_d phase and the dimmer regions correspond to the l_o phase due to selective partitioning of TopFluor PC; **B:** non-phase separated GUVs. It is assumed that the composition of these vesicles has changed and is not equal to the original intended composition.

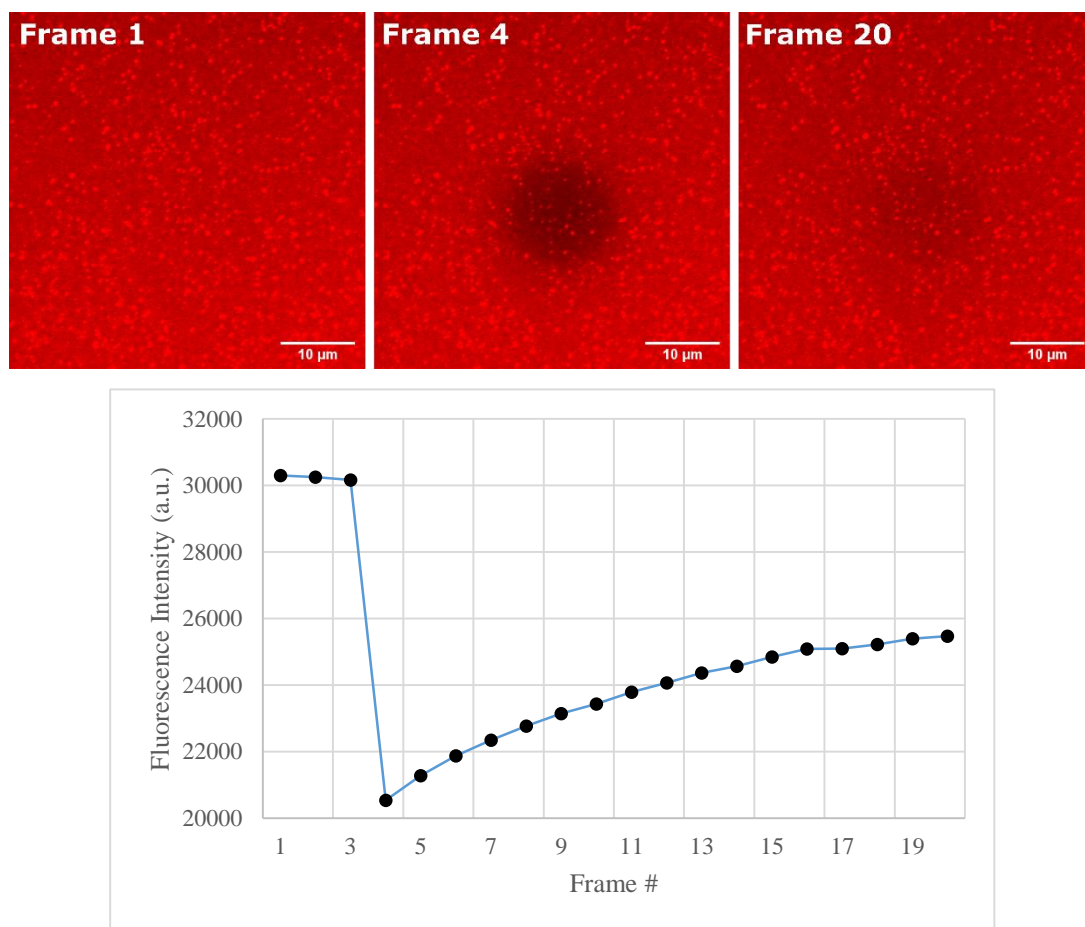


Figure 10. Supported lipid bilayer FRAP data. Top: FRAP images of an SLB formed from SUVs. Composition is 80% DOPC, 20% POPS, 0.2% Rhodamine-PE. Bottom: Corresponding fluorescence intensity data. Photobleaching occurred between capture of frames 3 and 4.

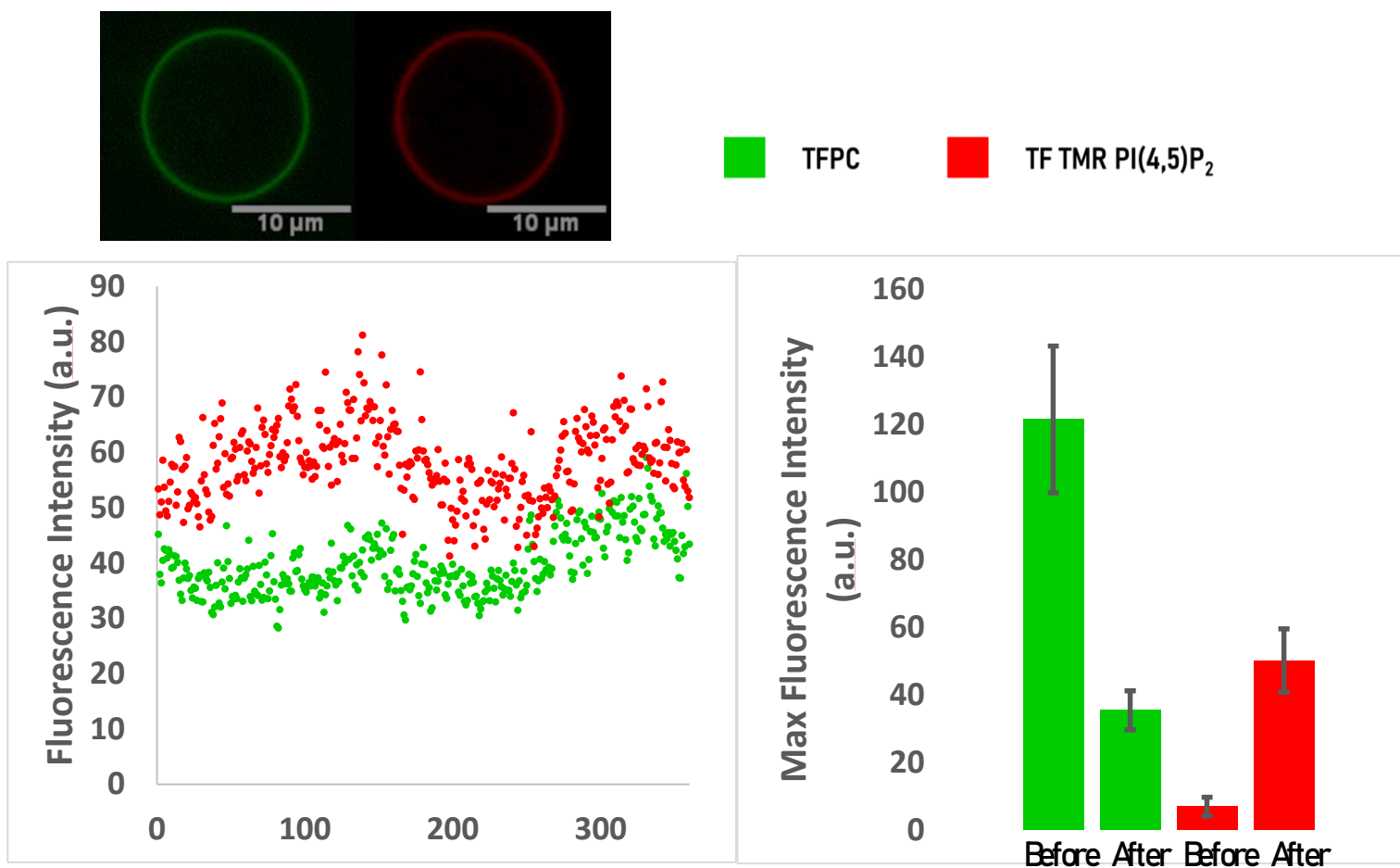


Figure 11. Quantification of asymmetry by fluorescence intensity in non-phase separated aGUVs. Intended inner leaflet composition: 40% DOPC, 40% DPPC, 20% cholesterol, 0.05% TopFluorPC. Outer leaflet composition: 90% DOPC, 10% PI(4,5)P₂, 0.1% TopFluor TMR PI(4,5)P₂. It is assumed that lipid composition in the inner leaflet has changed because phase separation did not occur. **Left:** a trace of the maximum fluorescence intensity of the aGUV bilayer along each degree of the circumference of a single aGUV (pictured above the graph). TopFluor PC (inner leaflet) shown in green; TopFluor TMR PI(4,5)P₂ (outer leaflet) shown in red. **Right:** Average maximum fluorescence intensity along the circumference of the bilayer of a population of aGUVs before and after hemifusion. Before n=34; after n=20. TopFluor PC (inner leaflet) shown in green; TopFluor TMR PI(4,5)P₂ (outer leaflet) shown in red.

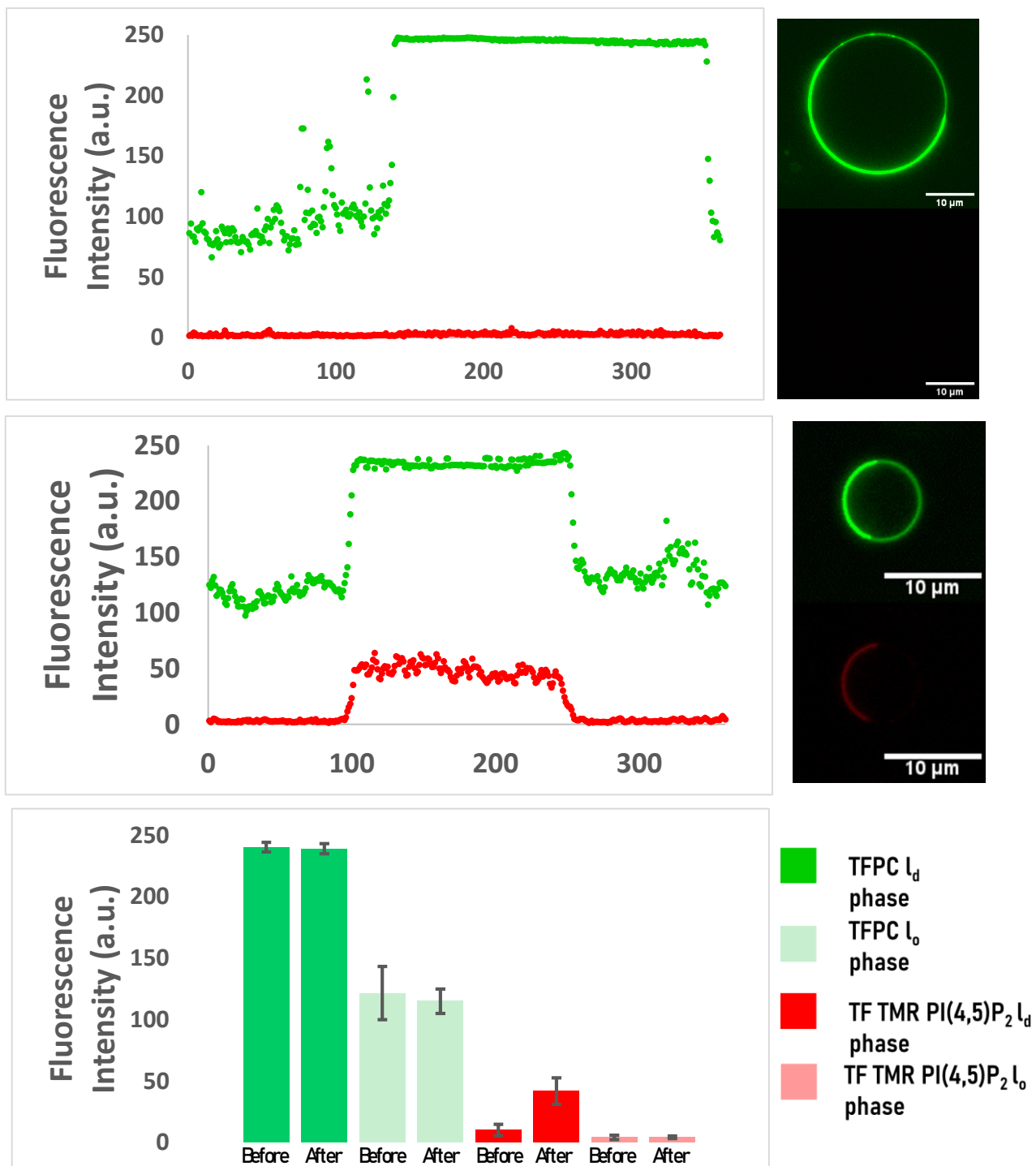


Figure 12. Quantification of asymmetry by fluorescence intensity in phase separated aGUVs. Inner leaflet composition: 40% DOPC, 40% DPPC, 20% cholesterol, 0.05% TopFluorPC outer leaflet composition: 90% DOPC, 10% PI(4,5)P₂, 0.1% TopFluor TMR PI(4,5)P₂. **Top:** a trace of the maximum fluorescence intensity of each degree around the circumference of a single symmetric GUV, before hemifusion (GUV pictured to the right of the graph). **Middle:** a trace of the maximum fluorescence intensity of each degree around the circumference of a single aGUV, after hemifusion (aGUV pictured to the right of the graph). TopFluor PC (inner leaflet) shown in green; TopFluor TMR PI(4,5)P₂ (outer leaflet) shown in red. **Bottom:** Average maximum fluorescence intensity along the circumference of the bilayer of a population of phase separated aGUVs before and after hemifusion. The average intensity of the l_o and l_d phases is separated to accurately represent the differing fluorescence intensity in each phase. Before n=34; after n=5. TopFluor PC (inner leaflet) shown in green; TopFluor TMR PI(4,5)P₂ (outer leaflet) shown in red.

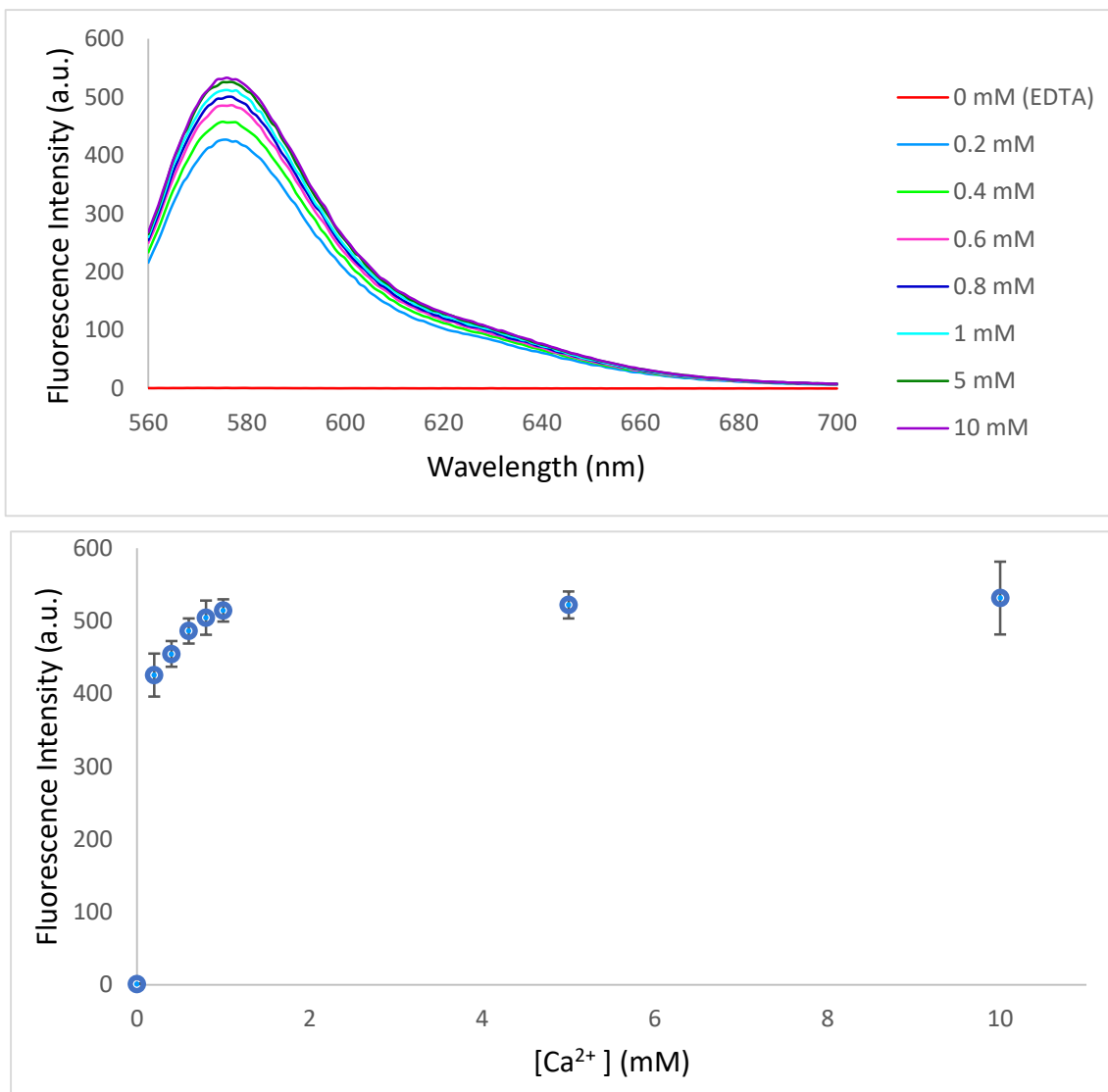


Figure 13. Calcium assay. Top: Fluorescence emission traces of 0.05 μM Rhod-5N with various concentrations of calcium. Rhod-5N exhibits a λ_{max} of 572 nm. **Bottom:** Standard curve of calcium concentrations measured at 572 nm.

Table 1. Various electroformation methods tested with DOPC^a in high salt buffer

#	Swelling Substrate	[NaCl] (mM)	Frequency	Voltage	Duration	Detachment
1	ITO coated slide	100	1 kHz	2.5 V ^b	2.5 hours	Pipetting
2	ITO coated slide	100	300 Hz	2 V ^c	2 hours	Pipetting
3	ITO coated slide	100	10 kHz	2.8 V ^b	2 hours	Pipetting
4	ITO coated slide	100	500 Hz	0.14 V – 3.25 V	Voltage increase over 30 min.; 90 min. at peak voltage	Frequency decrease from 500 Hz to 50 Hz over 30 minutes
5	Platinum wire	100	500 Hz	0.3 V – 7.8 V ^d	Voltage increase over 30 min.; 90 min. at peak voltage	Frequency decrease from 500 Hz to 50 Hz over 30 minutes
6	Platinum wire	100	1 kHz	5 V	2 hours	Pipetting
7	ITO coated slide	137 (PBS)	500 Hz	0.65 V – 4.175 V ^e	Voltage increase over 30 min.; Overnight at peak voltage (14-20 hours)	Frequency decrease from 500 Hz to 50 Hz over 30 minutes

^a Lipid mixture was DOPC with 0.2 % Rhodamine-PE. ^b As described by [49]. ^c As described by [49, 52]. ^d As described by [51]. ^e As described by [46].

References

1. Choy, C.H., B.K. Han, and R.J. Botelho, *Phosphoinositide Diversity, Distribution, and Effector Function: Stepping Out of the Box*. Bioessays, 2017. **39**(12).
2. Peres, C., et al., *Modulation of phosphoinositide 3-kinase activation by cholesterol level suggests a novel positive role for lipid rafts in lysophosphatidic acid signalling*. FEBS Lett, 2003. **534**(1-3): p. 164-8.
3. Arcaro, A., et al., *Critical role for lipid raft-associated Src kinases in activation of PI3K-Akt signalling*. Cell Signal, 2007. **19**(5): p. 1081-92.
4. Seveau, S., et al., *A FRET analysis to unravel the role of cholesterol in Rac1 and PI 3-kinase activation in the InlB/Met signalling pathway*. Cell Microbiol, 2007. **9**(3): p. 790-803.
5. Johnson, C.M., G.R. Chichili, and W. Rodgers, *Compartmentalization of phosphatidylinositol 4,5-bisphosphate signaling evidenced using targeted phosphatases*. J Biol Chem, 2008. **283**(44): p. 29920-8.
6. Furt, F., et al., *Polyphosphoinositides are enriched in plant membrane rafts and form microdomains in the plasma membrane*. Plant Physiol, 2010. **152**(4): p. 2173-87.
7. Das, S., S. Chakraborty, and A. Basu, *Critical role of lipid rafts in virus entry and activation of phosphoinositide 3' kinase/Akt signaling during early stages of Japanese encephalitis virus infection in neural stem/progenitor cells*. J Neurochem, 2010. **115**(2): p. 537-49.
8. Gao, X., et al., *PI3K/Akt signaling requires spatial compartmentalization in plasma membrane microdomains*. Proc Natl Acad Sci U S A, 2011. **108**(35): p. 14509-14.
9. Zhu, Y.Z., et al., *The role of lipid rafts in the early stage of Enterovirus 71 infection*. Cell Physiol Biochem, 2015. **35**(4): p. 1347-59.
10. Cizmecioglu, O., et al., *Rac1-mediated membrane raft localization of PI3K/p110beta is required for its activation by GPCRs or PTEN loss*. Elife, 2016. **5**.
11. Simons, K. and E. Ikonen, *Functional rafts in cell membranes*. Nature, 1997. **387**(6633): p. 569-72.
12. Cheng, H.T., Megha, and E. London, *Preparation and properties of asymmetric vesicles that mimic cell membranes: effect upon lipid raft formation and transmembrane helix orientation*. J Biol Chem, 2009. **284**(10): p. 6079-92.
13. Cheng, H.T. and E. London, *Preparation and properties of asymmetric large unilamellar vesicles: interleaflet coupling in asymmetric vesicles is dependent on temperature but not curvature*. Biophys J, 2011. **100**(11): p. 2671-8.
14. Enoki, T.A. and G.W. Feigenson, *Asymmetric Bilayers by Hemifusion: Method and Leaflet Behaviors*. Biophys J, 2019.
15. St Clair, J., et al., *"Preparation and Physical Properties of Asymmetric Model Membrane Vesicles" in "Springer Series in Biophysics: The Role of the Physical Properties of Membranes in Influencing Biological Phenomena" (Eds. R.M. Epand and J.M. Ruysschaert), Springer Press, in press. 2017. p. 1-27.*
16. Jiang, Z., et al., *Cholesterol stabilizes fluid phosphoinositide domains*. Chem Phys Lipids, 2014. **182**: p. 52-61.
17. Wen, Y., V.M. Vogt, and G.W. Feigenson, *Multivalent Cation-Bridged PI(4,5)P2 Clusters Form at Very Low Concentrations*. Biophys J, 2018. **114**(11): p. 2630-2639.
18. Singer, S.J. and G.L. Nicolson, *The fluid mosaic model of the structure of cell membranes*. Science, 1972. **175**(4023): p. 720-31.
19. Shevchenko, A. and K. Simons, *Lipidomics: coming to grips with lipid diversity*. Nat Rev Mol Cell Biol, 2010. **11**(8): p. 593-8.
20. van Meer, G., D.R. Voelker, and G.W. Feigenson, *Membrane lipids: where they are and how they behave*. Nat Rev Mol Cell Biol, 2008. **9**(2): p. 112-24.
21. Contreras, F.X., et al., *Transbilayer (flip-flop) lipid motion and lipid scrambling in membranes*. FEBS Lett, 2010. **584**(9): p. 1779-86.

22. Fadeel, B. and D. Xue, *The ins and outs of phospholipid asymmetry in the plasma membrane: roles in health and disease*. Crit Rev Biochem Mol Biol, 2009. **44**(5): p. 264-77.
23. Simons, K. and G. van Meer, *Lipid sorting in epithelial cells*. Biochemistry, 1988. **27**(17): p. 6197-202.
24. Lingwood, D. and K. Simons, *Lipid rafts as a membrane-organizing principle*. Science, 2010. **327**(5961): p. 46-50.
25. Levental, I. and S. Veatch, *The Continuing Mystery of Lipid Rafts*. J Mol Biol, 2016. **428**(24 Pt A): p. 4749-4764.
26. Munro, S., *Lipid rafts: elusive or illusive?* Cell, 2003. **115**(4): p. 377-88.
27. Curthoys, N.M., et al., *Dances with Membranes: Breakthroughs from Super-resolution Imaging*. Curr Top Membr, 2015. **75**: p. 59-123.
28. Levental, I., K.R. Levental, and F.A. Heberle, *Lipid Rafts: Controversies Resolved, Mysteries Remain*. Trends in Cell Biology, 2020.
29. Kinoshita, M., et al., *Raft-based sphingomyelin interactions revealed by new fluorescent sphingomyelin analogs*. J Cell Biol, 2017. **216**(4): p. 1183-1204.
30. Komura, N., et al., *Raft-based interactions of gangliosides with a GPI-anchored receptor*. Nat Chem Biol, 2016. **12**(6): p. 402-10.
31. Heberle, F.A., et al., *Direct label-free imaging of nanodomains in biomimetic and biological membranes by cryogenic electron microscopy*. bioRxiv, 2020: p. 2020.02.05.935551.
32. Feigenson, G.W., *Phase behavior of lipid mixtures*. Nat Chem Biol, 2006. **2**(11): p. 560-3.
33. Devaux, P.F. and R. Morris, *Transmembrane asymmetry and lateral domains in biological membranes*. Traffic, 2004. **5**(4): p. 241-6.
34. Takaoka, R., et al., *Formation of asymmetric vesicles via phospholipase D-mediated transphosphatidylation*. Biochim Biophys Acta Biomembr, 2018. **1860**(2): p. 245-249.
35. Chiantia, S., et al., *Asymmetric GUVs prepared by MbetaCD-mediated lipid exchange: an FCS study*. Biophys J, 2011. **100**(1): p. L1-3.
36. Hu, P.C., S. Li, and N. Malmstadt, *Microfluidic fabrication of asymmetric giant lipid vesicles*. ACS Appl Mater Interfaces, 2011. **3**(5): p. 1434-40.
37. Lin, Q. and E. London, *Preparation of artificial plasma membrane mimicking vesicles with lipid asymmetry*. PLoS One, 2014. **9**(1): p. e87903.
38. Chernomordik, L.V. and M.M. Kozlov, *Mechanics of membrane fusion*. Nat Struct Mol Biol, 2008. **15**(7): p. 675-83.
39. De Craene, J.O., et al., *Phosphoinositides, Major Actors in Membrane Trafficking and Lipid Signaling Pathways*. Int J Mol Sci, 2017. **18**(3).
40. Balla, T., *Phosphoinositides: tiny lipids with giant impact on cell regulation*. Physiol Rev, 2013. **93**(3): p. 1019-137.
41. Di Paolo, G. and P. De Camilli, *Phosphoinositides in cell regulation and membrane dynamics*. Nature, 2006. **443**(7112): p. 651-7.
42. McLaughlin, S., et al., *PIP(2) and proteins: interactions, organization, and information flow*. Annu Rev Biophys Biomol Struct, 2002. **31**: p. 151-75.
43. Laux, T., et al., *GAP43, MARCKS, and CAP23 modulate PI(4,5)P(2) at plasmalemmal rafts, and regulate cell cortex actin dynamics through a common mechanism*. J Cell Biol, 2000. **149**(7): p. 1455-72.
44. Lasserre, R., et al., *Raft nanodomains contribute to Akt/PKB plasma membrane recruitment and activation*. Nat Chem Biol, 2008. **4**(9): p. 538-47.
45. Chun, Y.S., et al., *Cholesterol modulates ion channels via down-regulation of phosphatidylinositol 4,5-bisphosphate*. J Neurochem, 2010. **112**(5): p. 1286-94.
46. Lefrancois, P., B. Goudeau, and S. Arbault, *Electroformation of phospholipid giant unilamellar vesicles in physiological phosphate buffer*. Integrative Biology, 2018. **10**(7): p. 429-434.
47. Angelova, M.I. and D.S. Dimitrov, *Liposome electroformation*. Faraday Discussions of the Chemical Society, 1986. **81**(0): p. 303-311.

48. Breton, M., M. Amirkavei, and L.M. Mir, *Optimization of the Electroformation of Giant Unilamellar Vesicles (GUVs) with Unsaturated Phospholipids*. J Membr Biol, 2015. **248**(5): p. 827-35.
49. Li, Q.C., et al., *Electroformation of giant unilamellar vesicles in saline solution*. Colloids and Surfaces B-Biointerfaces, 2016. **147**: p. 368-375.
50. Estes, D.J. and M. Mayer, *Giant liposomes in physiological buffer using electroformation in a flow chamber*. Biochimica Et Biophysica Acta-Biomembranes, 2005. **1712**(2): p. 152-160.
51. Pott, T., H. Bouvrais, and P. Meleard, *Giant unilamellar vesicle formation under physiologically relevant conditions*. Chem Phys Lipids, 2008. **154**(2): p. 115-9.
52. Stein, H., et al., *Production of Isolated Giant Unilamellar Vesicles under High Salt Concentrations*. Front Physiol, 2017. **8**: p. 63.
53. Larsen, J., N.S. Hatzakis, and D. Stamou, *Observation of Inhomogeneity in the Lipid Composition of Individual Nanoscale Liposomes*. Journal of the American Chemical Society, 2011. **133**(28): p. 10685-10687.
54. Morales-Pennington, N.F., et al., *GUV preparation and imaging: Minimizing artifacts*. Biochimica Et Biophysica Acta-Biomembranes, 2010. **1798**(7): p. 1324-1332.
55. Griko, Y.V., *Energetics of Ca²⁺-EDTA interactions: calorimetric study*. Biophysical Chemistry, 1999. **79**(2): p. 117-127.
56. Melcrova, A., et al., *The complex nature of calcium cation interactions with phospholipid bilayers*. Scientific Reports, 2016. **6**.
57. Magarkar, A., et al., *Increased Binding of Calcium Ions at Positively Curved Phospholipid Membranes*. Journal of Physical Chemistry Letters, 2017. **8**(2): p. 518-523.
58. Gericke, A., *Is Calcium Fine-Tuning Phosphoinositide-Mediated Signaling Events Through Clustering?* Biophys J, 2018. **114**(11): p. 2483-2484.
59. Carvalho, K., et al., *Giant unilamellar vesicles containing phosphatidylinositol(4,5)bisphosphate: characterization and functionality*. Biophysical journal, 2008. **95**(9): p. 4348-4360.
60. Beber, A., et al., *Septin-based readout of PI(4,5)P₂ incorporation into membranes of giant unilamellar vesicles*. Cytoskeleton (Hoboken), 2019. **76**(1): p. 92-103.